

UNIVERSITY OF CINCINNATI

Date: 05-13-2005

I, Zifei Liu,

hereby submit this work as part of the requirements for the degree of:
Master of Science

in:
Environmental Engineering

It is entitled:

The carbon and sulfur speciation of diesel emissions
from a non-road generator

This work and its defense approved by:

Chair: Dr. Mingming Lu

Dr. Tim C. Keener

Dr. Soon-Jai Khang

Dr. Paul Baron

The carbon and sulfur speciation of diesel emissions from a non-road generator

A thesis submitted to the
Division of the Research and Advanced Studies
of the University of Cincinnati

in partial fulfillment of the
requirements for the degree of

MASTER OF SCIENCE

in the Department of Civil and Environmental Engineering
of the College of Engineering

2005

by

Zifei Liu

B.S. Nanjing University, 1992

Committee Chair: Dr. Mingming Lu

ABSTRACT

The emissions of diesel particulate matter (DPM) from diesel engines are causing increasing health concerns due to their suspected carcinogenicity. DPM consists mostly of carbonaceous materials, which is often classified as elemental carbon (EC) and organic carbon (OC). EC and OC affect the environment in multiple ways due to their optical, physical, chemical, and toxicological properties. Sulfur species are also one of the important components in non-road diesel emissions. Especially, sulfate (SO_4^{2-}) is supposed to play an important role in particulate formation and organic compounds nucleation. This research investigated the distributions of carbon and sulfur speciation under various source conditions, and the study was performed on a non-road diesel generator.

For the study of carbon speciation, samples were collected using a EPA Method 5 sampling train, and OC/EC in DPM were measured by the thermal-optical method NIOSH 5040. Tests were performed at various engine loads, and the influence of diesel sulfur content and collection temperature on the OC/EC distributions were discussed. Results showed that DPM concentrations and the relative contributions of OC, EC, and other unaccounted mass vary greatly with engine load, fuel sulfur content, and sample collection temperature. The EC concentrations in DPM exhaust increase with increasing load, while the OC concentrations do not show great variation with load. It is also found that in the high sulfur diesel emissions both the OC and non-carbonaceous materials contribute more to DPM than in the low sulfur

diesel emissions. As expected, the collection temperature showed no influence on EC concentrations while it has a great influence on the OC and non-carbonaceous materials.

For the study of sulfur speciation, EPA Method 8 was utilized. DPM samples were collected at the same time as measuring sulfur dioxide (SO_2) and sulfuric acid (H_2SO_4) in emissions. Particulate sulfate (SO_4^{2-}) and Total particulate sulfur in DPM were determined by Ion Chromatography (IC) and X-Ray Fluorescence (XRF) spectroscopy analysis respectively. Results showed that, SO_2 concentration is clearly related to diesel sulfur content as well as engine load conditions in non-road diesel emissions. The $\text{S} \rightarrow \text{SO}_2$ conversion rates slightly decrease with increasing load. And they are obviously related with diesel types. For the same type of diesel, the conversion rates increase as diesel sulfur content increase. However, the total SO_4^{2-} concentration is not sensitive to diesel sulfur content. It is also found that the sulfur recovery is sensitive to diesel fuel types and may be related to the forms of sulfur compounds in diesel fuel.

Besides the study of carbon and sulfur speciation in DPM, an investigation of sampling artifacts was performed on a high volume sampling system. Quartz pair tandem filters were used in the tests, and DPM influenced samples were collected at two different filter face velocities and a series of collection time. It is found that, under the specified sampling conditions in the study, OC on the backup filter was

mainly from adsorption of vapor but not from volatilization of particles on front filter. The quartz-quartz pair tandem filter method can be used to correct the adsorption artifacts by subtracting backup filter measurements from the front filter measurements. However the accuracy of the method improves with increased collection time. In order to effectively correct the adsorption artifacts, collection time should be long enough to approach gas/filter adsorption equilibrium. The study also estimated the capability of the applied quartz filter to adsorb OC vapor and found that it was not obviously influenced by sampling face velocity. The information will be helpful to choose valid sampling duration time for field sampling in order to effectively correct sampling artifacts caused by adsorption.

ACKNOWLEDGEMENTS

I would like to thank my advisor, Dr. Mingming Lu, for her guidance, instructions and encouragement through out my research. I also want to thank Dr. Tim C. Keener, Dr. Soon-Jai Khang and Dr. Paul Baron for their valuable suggestions and support.

Fuyan Liang, Prabhat Lamichhane and Phirun Saiyasitpanich provided great assistance in sampling and analysis work in this study, and I am grateful for their help.

Financial support from National Institute for Occupational Safety and Health (NIOSH) is gratefully acknowledged.

TABLE OF CONTENTS

LIST OF FIGURES	4
LIST OF TABLES	6

Chapter 1 Introduction

1.1 Background	7
1.1.1 Characterization of DPM	7
(1) Compositions of DPM	7
(2) DPM size distributions	7
(3) DPM dynamics	9
(4) Review of monitoring methods of DPM	9
1.1.2 Health concerns of DPM	10
1.1.3 Non-road diesel emissions	10
1.2 Research objectives	11
1.3 Reference	12

Chapter 2 Investigation of OC/EC Distribution in DPM from a Non-road Diesel Generator

2.1 Introduction	15
2.2 Experimental methods	15
2.2.1 Experimental setup	15
2.2.2 Sampling method (Modified EPA Method 5)	16
2.2.3 OC/EC analysis (Thermal-optical method NIOSH 5040)	17
2.2.4 Sampling artifacts	18
2.3 Results and discussions	19
2.3.1 Overall trend of OC/EC distribution with Load	19
2.3.2 Influence of the sulfur content in diesel fuels	21
2.3.3 Influence of DPM collection temperatures	24

2.4 Conclusion	27
2.5 References	28

Chapter 3 Investigation of Sulfur Species Distribution in Non-road Diesel Emissions

3.1 Introduction	30
3.2 Experimental methods	30
3.3 Results and discussions	31
3.3.1 SO ₂	31
(1) Measured SO ₂ concentration	31
(2) Theoretical SO ₂ concentrations	32
3.3.2 SO ₄ ²⁻	35
3.3.3 Particulate sulfur	40
3.3.4 Sulfur balance and recovery	42
3.4 Conclusion	43
3.5 References	44

Chapter 4 Investigation of Organic DPM Sampling Artifacts of a High-volume Sampling System

4.1 Introduction	47
4.1.1 Sampling artifacts of organic aerosol	47
4.1.2 Tandem filter method for correcting artifacts	47
4.1.3 Equilibrium between gas and adsorbed phases	48
4.1.4 Measurement of OC in DPM	49
4.2 Objective of the study	50
4.3 The high volume sampling system	50
4.3.1 Development of the high volume sampling system	50
4.3.2 Calibration of the flow rate	51
4.4 Experimental methods	54
4.5 Results and discussions	55

4.5.1 Measurements of EC	55
4.5.2 Dependency of OC measurements on collection time	56
4.5.3 Dependency of OC measurements on face velocity	58
4.5.4 Corrected OC concentrations	59
4.5.5 The gas/filter adsorption equilibrium	60
4.6 Conclusion	62
4.7 References	63
Chapter 5 Recommendations for Future Work	65

Appendix A: Data sheet of OC/EC study in Chapter 2

Appendix B: Data sheet of sulfur speciation study in Chapter 3

Appendix C: Data sheet of sampling artifacts study in Chapter 4

Appendix D: SEM images of DPM

LIST OF FIGURES

Figure 1-1 Typical structure of DPM (Kittelson, 1998a)

Figure 1-2 Typical engine exhaust DPM size distributions (Kittelson, 1998a)

Figure 2-1 Experimental setup

Figure 2-2 Thermogram for the thermal-optical method NIOSH 5040

Figure 2-3 Concentration of OC, EC, and DPM vs. engine load (Sulfur content = 500ppm; collection temperature = $120\text{ }^{\circ}\text{C} \pm 14\text{ }^{\circ}\text{C}$; error bars correspond to range of concentration measurements; $n = 5, 7, 5, 4$ at 0 kW, 25 kW, 50 kW, and 75 kW, respectively)

Figure 2-4 Fractions of organic compounds, EC and unaccounted mass in DPM vs. load (Sulfur content = 500ppm, Collection temperature = $120 \pm 14\text{ }^{\circ}\text{C}$)

Figure 2-5 Concentration of OC, EC, and DPM vs. engine load (Sulfur content = 3700ppm, collection temperature = $120\text{ }^{\circ}\text{C} \pm 14\text{ }^{\circ}\text{C}$)

Figure 2-6 Fractions of organic compounds, EC, and unaccounted mass in DPM vs. load (Sulfur content = 3700ppm, collection temperature = $120\text{ }^{\circ}\text{C} \pm 14\text{ }^{\circ}\text{C}$)

Figure 2-7 Ratios of organic compounds, EC, and unaccounted mass concentrations in the high sulfur diesel (sulfur content = 3700ppm) emissions over those in the low sulfur diesel (sulfur content = 500ppm) emissions. Collection temperature = $120\text{ }^{\circ}\text{C} \pm 14\text{ }^{\circ}\text{C}$ for both.

Figure 2-8 OC/EC vs. load (S = sulfur content, collection temperature = $120\text{ }^{\circ}\text{C} \pm 14\text{ }^{\circ}\text{C}$)

Figure 2-9 Fractions of organic compounds, EC, and unaccounted mass in DPM vs. load (Sulfur content = 500ppm, collection temperature = $25\text{ }^{\circ}\text{C} \pm 3\text{ }^{\circ}\text{C}$)

Figure 2-10 Ratios of organic compounds, EC, and unaccounted mass concentrations for a collection temperature of $25\text{ }^{\circ}\text{C} \pm 3\text{ }^{\circ}\text{C}$ over that for a collection temperature of $120\text{ }^{\circ}\text{C} \pm 14\text{ }^{\circ}\text{C}$ (sulfur content = 500ppm)

Figure 2-11 OC/EC vs. load (Sulfur content = 500ppm, T = temperature)

Figure 3-1 SO_2 concentrations

Figure 3-2 S to SO₂ conversion rates
Figure 3-3 Total SO₄²⁻ concentrations
Figure 3-4 S to SO₄²⁻ conversion rates
Figure 3-5 Diesel consumption rates
Figure 3-6 S to SO₄²⁻ conversion rate vs. excess air
Figure 3-7 Vapor phase SO₄²⁻ /Total SO₄²⁻
Figure 3-8 Total particulate sulfur concentrations
Figure 3-9 S to total particulate sulfur (TPS) conversion rates
Figure 3-10 Particulate Sulfate-S/TPS ratio under various loads
Figure 3-11 Sulfur recovery

Figure 4-1 The high-volume sampling system
Figure 4-3 Calibration curve of the three high volume samplers
Figure 4-3 Picture of the high volume sampling system and the DPM emission source
Figure 4-4 Apparent OC and EC concentrations based on the front filter measurement at 105cm/s face velocity
Figure 4-5 Normalized apparent concentrations of OC based on the front filter measurement at the two different face velocities
Figure 4-6 Normalized concentrations of OC vapor adsorbed on the backup filter at the two different face velocities
Figure 4-7 Corrected OC concentration by subtracting backup filter measurements from the front filter measurements at the two different face velocities
Figure 4-8 The difference of corrected OC at the two different face velocities [(OC at v=80cm/s)-(OC at v=105cm/s)]
Figure 4-9 OC loading (before normalization) on the backup filter along with the collection time
Figure 4-10 OC loading on the filter along with the collection time in the Method 5 test

LIST OF TABLES

Table 2-1 OC/EC distributions reported by different researchers

Table 3-1 Comparison of the theoretical and the measured SO₂ concentration

Table 4-1 Parameters of flow rate calibration

Table 4-2 Calibration data of three high volume samplers

1.1 Background

1.1.1 Characterization of DPM

(1) Compositions of DPM

Diesel particulate matter (DPM) is a complex mixture of organic and inorganic compounds that exist in particle phase. The organic compounds appear as volatile or soluble organic and are generally described as the soluble organic fraction (SOF). SOF contains polycyclic aromatic compounds and can also contain hetero-atoms such as oxygen, nitrogen, and sulfur (1). Some organic compounds are generated from unburned fuel and evaporated lube oil, and some may be formed during combustion or reaction with catalysts. The inorganic compounds are primarily formed during combustion process. Carbon in the fuel is mostly oxidized in the form of solid carbon particles (SOL) or soot. Sulfur in the fuel is mostly oxidized to SO_2 , but a small fraction is oxidized to SO_3 that leads to sulfuric acid and sulfate aerosol. Metal compounds in fuel and lube oil lead to a small amount of inorganic ash. DPM consists mainly of highly agglomerated SOL and ash, SOF and sulfate particles. DPM may also be associated with liquid condensed or adsorbed hydrocarbons. Figure 1-1 shows the typical structure of DPM (Kittelson, 1998a)

(2) DPM size distribution

Size distribution of DPM is influenced by many factors, such as fuel properties, engine operating conditions, and the conditions when it is collected, etc. Kittelson studied DPM size distributions of typical engine exhaust (1). Figure 1-2 shows the idealized diesel aerosol number and mass weighted size distributions (Kittelson, 1998a). The distributions are lognormal in form. Most of the particle mass exists in the accumulation mode (the 0.05 to 1.0 μm diameter range), while 90 % of the particle number exists in the nuclei mode (the 0.005 to 0.05 μm diameter range). It is believed that, the accumulation mode is where the carbonaceous agglomerates and associated adsorbed materials reside,

and the nuclei mode usually consists of volatile organic and sulfur compounds that form during exhaust dilution and cooling, and may also contain solid carbon and metal compounds.

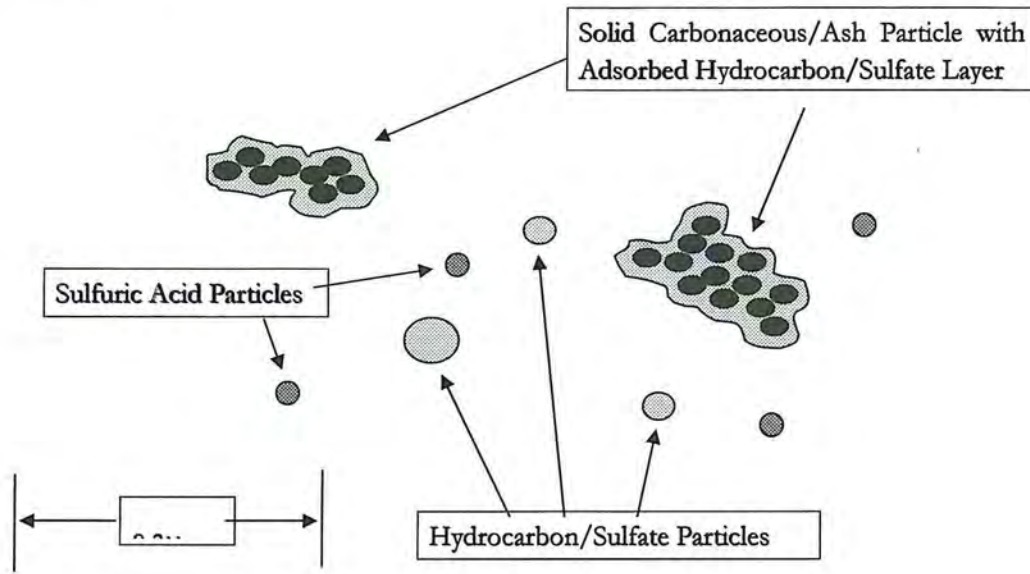


Figure 1-1 Typical structure of DPM (Kittelson, 1998a)

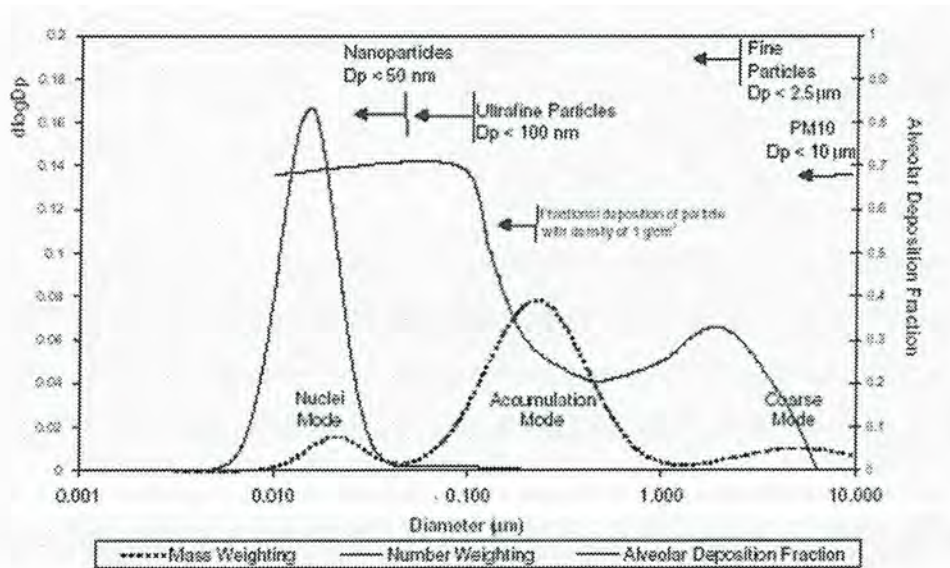


Figure 1-2 Typical engine exhaust DPM size distributions (Kittelson, 1998a)

(3) DPM dynamics

DPM dynamics and transformations greatly impact the measurement of DPM. These processes include coagulation, nucleation, adsorption/desorption, and condensation/evaporation. Both the characteristics of the engine emissions and the environmental conditions may influence the nature of the measurement (2). These factors include: size, number, and composition of particles emitted from the engine; composition and quantity of volatile particle precursors in the exhaust; dilution ratio; residence time; humidity and temperature; background particle and gas concentrations, etc.

As engine exhaust is diluted and cooled, SOF, the soluble organic fraction, may move from the gas phase to the particle phase by two paths: adsorption on or absorption into existing particles or nucleation to form new particles. Carbonaceous agglomerates in DPM have large surface areas available for adsorption of volatile materials. Also, it has been observed in diesel exhaust that volatile organic matter can nucleate and grow to form nuclei mode particles at saturation values below supersaturation. There are heterogeneous nuclei present in diesel exhaust in the form of sulfuric acid and possibly metallic ash (2). Analysis for organic carbon (OC) showed that the dilution stack sampler collected 7-16 times as much organic aerosol as the non-dilution method called EPA Method 5 (3).

(4) Review of monitoring methods of DPM

Measuring diesel aerosol in the workplace is challenging due to the physical characteristics and chemical complexity of the aerosol. Three methods are routinely used in mines to quantify the DPM exposure: the respirable combustible dust method (RCD), the size selective method (SS), and the elemental carbon method (EC) (4).

RCD and SS are gravimetric method. In the RCD method, a personal sampling pump passes the gas through a cyclone, which acts as a respirable dust pre-classifier with a cut point of 4.0 μm . In the SS method, a personal sampling pump draws air through a

cyclone followed by an inertial impactor with a 0.8 μm cut point. In the EC method, samples are collected with or without an inertial pre-selector to remove larger particles followed by carbonaceous analysis, and EC portion of sample is regarded as a specific marker of DPM. Each of these methods measures a different portion of DPM.

1.1.2 Health concern of DPM

The emissions of DPM from diesel engines are causing increasing health concerns due to their suspected carcinogenicity, especially the carbonaceous fractions. DPM consists mostly of carbonaceous materials, which is often classified as elemental carbon (EC) and organic carbon (OC). EC and OC affect the environment in multiple ways due to their optical, physical, chemical, and toxicological properties. EC, the diesel soot particle's core, is a byproduct of incomplete combustion consisting of carbon layers that are structurally similar to graphite. Particulate OC consists of liquid droplets and soot-associated organics. The OC fraction of DPM is a complex mixture of unburned fuel, oil, and numerous organic compounds including PAHs (polycyclic aromatic hydrocarbons). EC has been linked to dysrhythmia and cardiovascular diseases (5), while PAHs in OC fraction are reasonably anticipated to be human carcinogens (6-7). These PAHs, when adsorbed on particle surfaces, can be detrimental to human health as 90% of the DPM particles are in the respirable size range of less than 1.0 μm (8). The National Institute for Occupational Safety and Health (NIOSH) considers diesel exhaust a potential occupational carcinogen⁶. Other organizations, including the International Agency for Research on Cancer (IARC) (9), the World Health Organization (WHO) (10), the California Environmental Protection Agency (6), the U.S. EPA (11), and the National Toxicology Program (12) have reviewed the animal and human evidence, and each has classified diesel exhaust as a probable human carcinogen or similar designation.

1.1.3 Non-road diesel emissions

Non-road diesel engines are widely used in construction, mining, agriculture, marine vessels, locomotives, and power equipment at various capacities and operating conditions.

However, the emissions from them are not as well characterized as those from on-road diesel vehicles. U.S. Environmental Protection Agency (EPA) studies indicated that emissions of diesel particulate matter (DPM) from non-road diesel machines are significantly higher than those from on-road sources because of lower fuel quality, inadequate engine maintenance, older engine age, etc. The engineering and production costs of developing new non-road emission reduction technologies are generally higher than those for on-road equipment due to the technical complexities, yet these costs must be distributed among a much lower production volume. Non-road diesel machines currently account for approximately 44% of total DPM and 12% of NO_x emissions from mobile sources nationwide (13). In the United States, the reported five-year sales volume of generator sets of sizes between 56 and 130 kW from the years 1996 to 2000 totaled 103,490 units (14). As for the diesel consumption, from source of Department of Energy, it is known that, Off-highway diesel occupy 9% of total Petroleum consumption.

It is believed that increased fuel sulfur content can result in increased DPM emissions (15). On May 11, 2004, the U.S. EPA announced a comprehensive rule to reduce emissions from non-road diesel engines by integrating engine and fuel controls as a system to gain the greatest emission reductions. This rule will decrease the current sulfur levels in non-road diesel fuels from about 3000ppm to 15ppm when fully implemented (a reduction of greater than 99 percent), and therefore will dramatically influence the characterization of emissions (16).

1.2 Research objective

The study is focused on the characterization and measurement of DPM, and it includes the following three parts:

(1) Investigation of OC/EC Distribution in DPM from a Non-road Diesel Generator

As we know, DPM consists mostly of carbonaceous materials, about 70% to 88%, which is often classified as EC and OC. EC and OC affect the environment in different ways

due to their different properties. The objective of the study is to provide a detailed account of the OC/EC distribution for a non-road diesel generator at various engine loads. And the influences of diesel sulfur content and collection temperature on the OC/EC distributions were discussed.

(2) Investigation of Sulfur Species Distribution in Non-road Diesel Emissions

Sulfur species are one of the major components in non-road diesel emissions. Sulfur dioxide (SO_2) is a primary pollutant, and sulfate (SO_4^{2-}) is supposed to play an important role in particulate formation and organic compounds nucleation (17). The objective of this study is to provide a detailed account of the sulfur species distributions for a diesel generator under various load conditions and to obtain a sulfur balance. Relationship between sulfur content in diesel and distribution of sulfur species in diesel emissions were established. The sensitivity of sulfur species to fuel sulfur level under various engine load conditions was studied.

(3) Investigation of Organic DPM Sampling Artifacts of a High-volume Sampling System

Organic compounds constitute approximately 20% to 60% of DPM. However, filter collection of organic compounds in DPM is often complicated by sampling artifacts. The third part of my study is to investigate the sampling artifacts in organic DPM measurement for a high-volume application. Experiments are designed to evaluate the relative magnitude of adsorption and volatilization sampling artifacts. Based on the experimental results, the study also tries to determine the minimum sampling volume (sampling duration time) required to attain organic gas-phase adsorbed-phase equilibrium on a previously clean quartz fiber filter. The information will be helpful to choose valid sampling duration time for field sampling in order to effectively correct sampling artifacts caused by adsorption.

1.3 Reference

- (1) Kittelson, D.B; Arnold, M.; Watts, W.F. Diesel Exhaust Particle Measurement Instruments – Supplemental Report No.1 for EPA Grant Review of Diesel Particulate Matter Sampling Methods, 1998a
- (2) Kittelson, D.B; Arnold, M.; Watts, W.F. Review of Diesel Particulate Matter Sampling Methods, Final Report, 1999
- (3) Hildemann, L.M.; Cass, G.R.; Markowski, G.R. A dilution stack sampler for collection of organic aerosol emissions: design, characterization and field tests, *Aeros. Sci. And Techno.* Vol. 10, 193-204, 1989
- (4) Watts, W.F. Jr., Diesel Particulate Matter Sampling Methods: Statistical Comparison, *Final Report Submitted to the Diesel Emission Evaluation Program*
- (5) Tolbert, P.E.; Klein, M.; Metzger, K.B.; Peel, J.; Flanders, W.D.; Todd, K.; Mulholland, J.A.; Ryan, P.B.; Frumkin, H. Interim results of the study of particulates and health in Atlanta (SOPHIA). *J. Expos. Anal. Environ. Epidemiol.* 2000, 10, 446-460
- (6) California Environmental Protection Agency. Proposed identification of diesel exhaust as a toxic air contaminant: health risk assessment for diesel exhaust. Office of Environmental Health Hazard Assessment, Sacramento, CA, 1998.
- (7) Truex, T.J.; Norbeck, J.M.; Smith, M.R. Evaluation of factors that affect diesel exhaust toxicity. Submitted to California Air Resources Board. Center for Environmental Research and Technology, University of California, Riverside, CA. 1998.
- (8) Watts, W.F., Jr.; Ramachandran, G. Diesel particulate matter sampling methods: statistical comparison. Final report submitted to the diesel emission evaluation program, University of Minnesota, November, 2000.
- (9) International Agency for Research on Cancer, IARC monographs on the evaluation of carcinogenic risks to humans: diesel and gasoline engine exhausts and some nitroarenes. Lyon, France, v. 46, p. 458. 1989.
- (10) World Health Organization, Diesel fuel and exhaust emissions. Environmental Health Criteria 171; Geneva, Switzerland, 1996.

- (11) U.S. Environmental Protection Agency, Health assessment document for diesel emission. Review Draft EPA/600/8-90/057E; National Center for Environmental Assessment; Washington, DC, 2000.
- (12) National Toxicology Program, Ninth Report on Carcinogens, Research Triangle Park, NC, 2000.
- (13) U.S. Environmental Protection Agency, Reducing air pollution from nonroad engines. EPA420-F-03-011; Office of Transportation and Air Quality; April 2003.
- (14) U.S. Environmental Protection Agency, Nonroad engines, equipment, and vehicles; reducing nonroad diesel emissions; industry characterization. Available at <http://www.epa.gov/nonroad/r03008b.pdf> (accessed 2004).
- (15) Corro, G. Sulfur Impact on Diesel Emission Control - A Review, *React.Kinet.Catal.Lett.* Vol. 75, No. 1, 89-106, 2002
- (16) U.S. EPA, Office of Transportation and Air Quality, Regulatory Announcement, EPA420-F-04-032, May 2004
- (17) Shi, J.P.; Harrison, R.M. Investigation of Ultrafine Particle Formation during Diesel Exhaust Dilution, *Environ. Sci. Technol.* Vol. 33, 3730-3736, 1999

Chapter 2 Investigation of OC/EC Distribution in DPM from a Non-road Diesel Generator

2.1 Introduction

EC and OC contributions to DPM vary, depending upon a number of factors, such as the fuel type, engine type, duty cycle, engine maintenance, individual operators, the use of emission control devices, and the compositions of the lubricant oil. There have been some previous studies on the OC/EC variation with load conditions for new heavy duty diesel vehicles (1) and military vehicles (2), but information is scarce for non-road diesel generators. The objective of the study is to provide a detailed account of the OC/EC distribution for a non-road diesel generator operated with high and low sulfur fuels under different load conditions. Total DPM concentrations are also reported. Samples were collected at two different temperatures to determine the influence of temperature on the OC/EC distributions and total DPM.

2.2 Experimental methods

2.2.1 Experimental setup

The study was performed on a Generac diesel generator (Model SD080, 5.0 Direct-Injection, Turbo charging, and Compression-Ignition) rated at 80 kW and 1800 rpm. A load simulator (model Merlin 100 by Simplex) was used to simulate various load conditions from 0 kW to 75 kW. DPM was collected on quartz fiber filters (Millipore) with EPA Method 5 (Determination of Particulate Matter Emissions from Stationary Sources) (3) sampling train. The applied engine load ranged from 0 kW to 75 kW with 25 kW increments. The DPM mass concentrations were determined by gravimetric analysis. Before being weighed, filters were desiccated at 20 ± 5.6 °C and ambient pressure for at least 24 hours. The OC/EC loadings on the filters were determined by NIOSH 5040, a thermal-optical analysis method commonly used in North America for OC/EC measurement (4). Two diesel fuels with different sulfur contents (500ppm and 3700ppm by weight respectively) were used in the study to evaluate the potential influence of fuel

sulfur content on the OC/EC distribution in DPM.

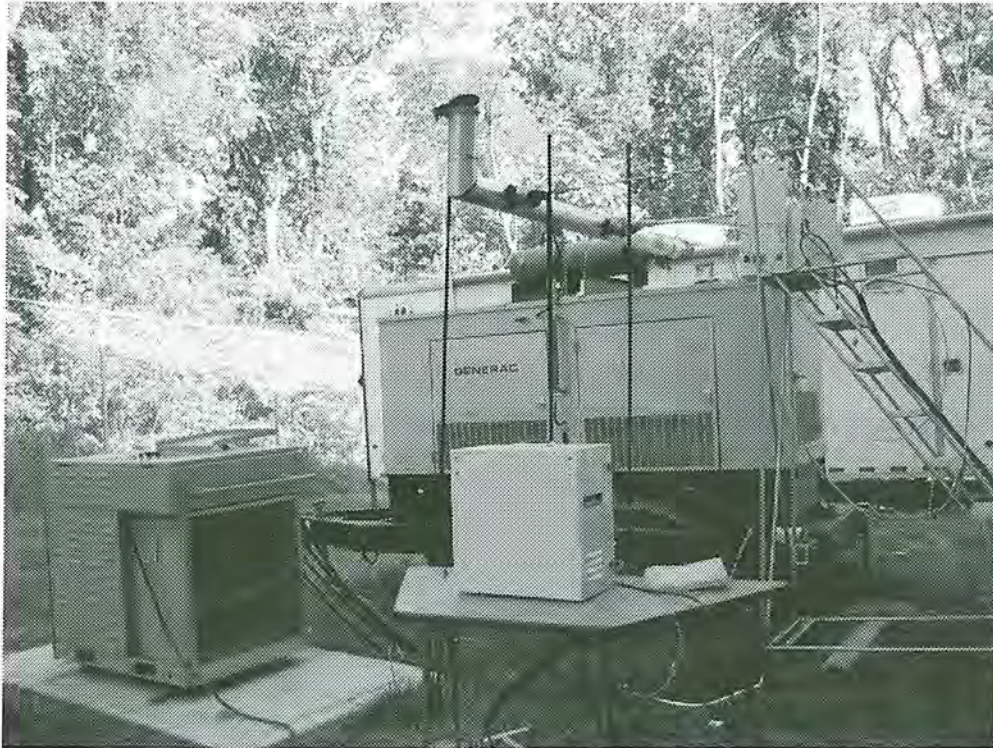


Figure 2-1 Experimental setup

2.2.2 Sampling method (Modified EPA Method 5)

In EPA Method 5, the undiluted exhaust is sampled through a heated sampling probe. Particulate matter is withdrawn isokinetically from the source and collected on a glass fiber filter maintained at $120 \pm 14^{\circ}\text{C}$. The particulate mass, which includes any material that condenses at or above the collection/filtration temperature, is determined gravimetrically after the removal of uncombined water.

For the measurement of OC/EC concentrations, the following two modifications were made to the EPA Method 5 sampling procedures for practical purposes: (a) particles were collected on quartz fiber filters instead of glass fiber filters as quartz filters are required for thermal-optical analysis by NIOSH 5040(4); (b) due to the maximum loading limitation of the OC/EC analysis, the sampling duration for DPM collection ranged from about 8 to 15 minutes, which is much shorter than a typical Method 5 sampling period of

approximately 60 minutes.

The gas-particle partitioning of the organic components of diesel exhaust emissions is sensitive to changes in temperature and pressure. As already mentioned, in EPA Method 5, the filter is heated and the DPM collection temperature is maintained at 120 ± 14 °C to prevent condensation of water, which also results in evaporation of semi-volatile organic compounds (SVOC). On the other hand, the filters are not heated in most DPM collection systems employing dilution methods under ambient conditions. To better understand the influence of collection temperature, a comparison group of samples was collected. In this group of samples, the filter was not heated and the collection temperature was maintained at 25 ± 3 °C.

2.2.3 OC/EC analysis (Thermal-optical method NIOSH 5040)

The thermal-optical method NIOSH 5040 (4) is most commonly used in North America for OC/EC analysis. In the method, speciation of OC and EC is accomplished through temperature and atmosphere control, and by continuous monitoring of filter transmittance. Laser light passed through the filter allows continuous monitoring of filter transmittance. Because temperatures in excess of 850 °C are employed during the analysis, quartz-fiber filters are required. A punch from the sample filter is taken for analysis, and OC and EC are reported in terms of μg per cm^2 of filter area. The total OC and EC on the filter are calculated by multiplying the reported values by the deposit area. In this approach, a homogeneous sample deposit is assumed.

Thermal-optical analysis proceeds essentially in two stages. In the first, organic and carbonate (if present) carbon are evolved in a helium atmosphere as the temperature is stepped to about 850°C. The evolved carbon is catalytically oxidized to CO_2 in a bed of granular MnO_2 , then reduced to CH_4 in a Ni/firebrick methanator. CH_4 is quantified by an FID. In the second stage, the sample oven temperature is reduced, an oxygen-helium

mix is introduced, and the temperature is stepped (to about 940°C). As oxygen enters the oven, pyrolytically generated carbon (PC) is oxidized and a concurrent increase in filter transmittance occurs (see Figure 2-2). The point at which the filter transmittance reaches its initial value is defined as the "split" between OC and EC. Carbon evolved prior to the split is considered OC (including carbonate), and carbon volatilized after the split is considered EC. TC is the sum of OC and EC. Like all OC/EC methods, the thermal-optical method is an operational method in the sense that the analytical procedure itself defines the analyte.

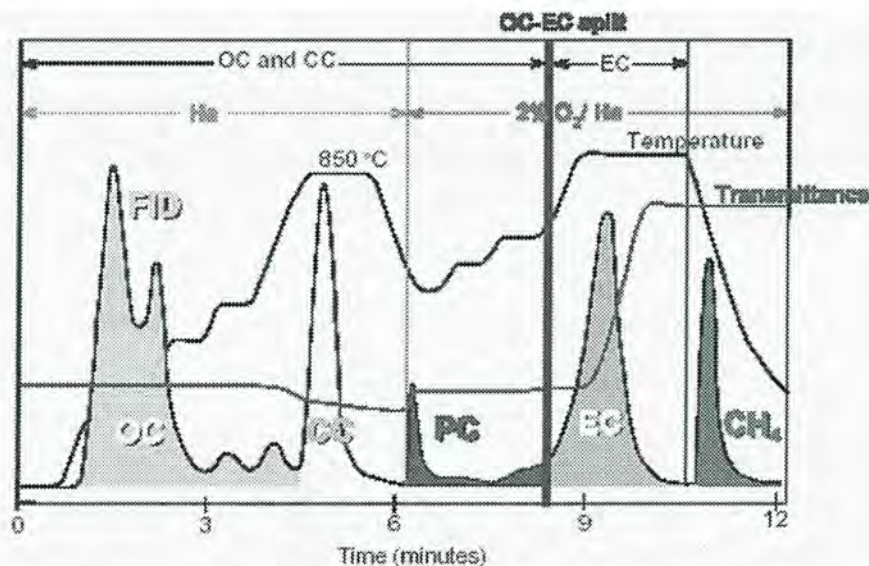


Figure 2-2 Thermogram for the thermal-optical method NIOSH 5040

2.2.4 Sampling artifacts

Quartz-quartz tandem filter method was tried to estimate the OC sampling artifacts. Results showed that, the backup filter can collect 13.15% to 31.42% of OC that were collected on the front filter. For the same engine load, the percentage decreases as sampling collection time increases. For the same sampling collection time, the percentage decreases as engine load increase. Since the artifacts is complicated with sampling conditions and it is not well known that if most of the adsorbed OC on backup filter was initially present in the vapor phase, or if it was from volatilization of particles collected

on the front filter, no corrections were made to the OC in this study as what Cadle did in his paper (5).

2.3 Results and discussions

2.3.1 Overall Trend of OC/EC Distribution with Load

Figure 2-3 presents the OC, EC, and DPM concentrations for low sulfur diesel (fuel sulfur content at 500ppm) emissions collected at 120 ± 14 °C under various loads. The data indicate that the EC concentrations increase by a factor of about 15 when going from 0 kW to 75 kW loads. Similarly, DPM also increases with load. The increase in EC concentrations with load is consistent with the higher fuel usage, less air and higher temperature at higher loads, as EC is a product of incomplete combustion (6). At higher load conditions, the increase in EC is more rapid than at lower loads. In contrast, the OC concentrations exhibit much less variation with load. Therefore, OC/EC ratios decrease with increasing load.

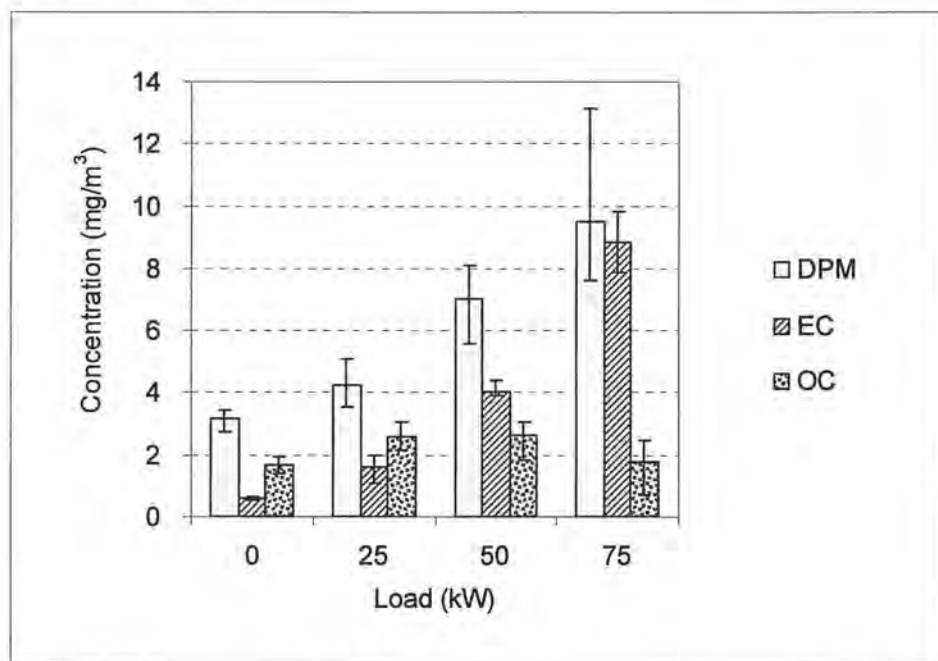


Figure 2-3 Concentration of OC, EC, and DPM vs. engine load (Sulfur content = 500ppm; collection temperature = 120 °C \pm 14 °C; error bars correspond to range of concentration measurements; $n = 5, 7, 5, 4$ at 0 kW, 25 kW, 50 kW, and 75 kW, respectively)

DPM can be classified into three portions: organic compounds, EC, and unaccounted mass. The mass concentration of organic compounds can be estimated from OC by a multiplicative factor of 1.2 to account for other elements, (e.g., hydrogen, oxygen, nitrogen, sulfur) in addition to carbon (7). The unaccounted mass may include sulfates, nitrates, metals, and ash, which were indirectly measured by the difference between DPM and the carbonaceous mass fractions (i.e., the total mass of EC and the organic compounds).

The fractions of organic compounds, EC, and unaccounted mass in DPM at various loads for the low sulfur diesel fuel and a collection temperature of $120\text{ }^{\circ}\text{C} \pm 14\text{ }^{\circ}\text{C}$ are shown in Figure 2-4. It is seen that the EC content increases from 21% at 0 kW to 84% at 75 kW, while the fraction of organic compounds decreases from 62% at 0 kW to 9% at 75 kW. These results are consistent with studies by Shi *et al.* (1) and Burtscher *et al.* (8). Shi *et al.*(1) reported that EC fractions increase by a factor of about 1.5 and OC fractions decrease by a factor of about 2 when increasing the load on a diesel engine from 25% to 100%. Burtscher *et al.* (8) reported that the volatile fraction decreased significantly with increasing load while the black-carbon concentration increased with increasing load.

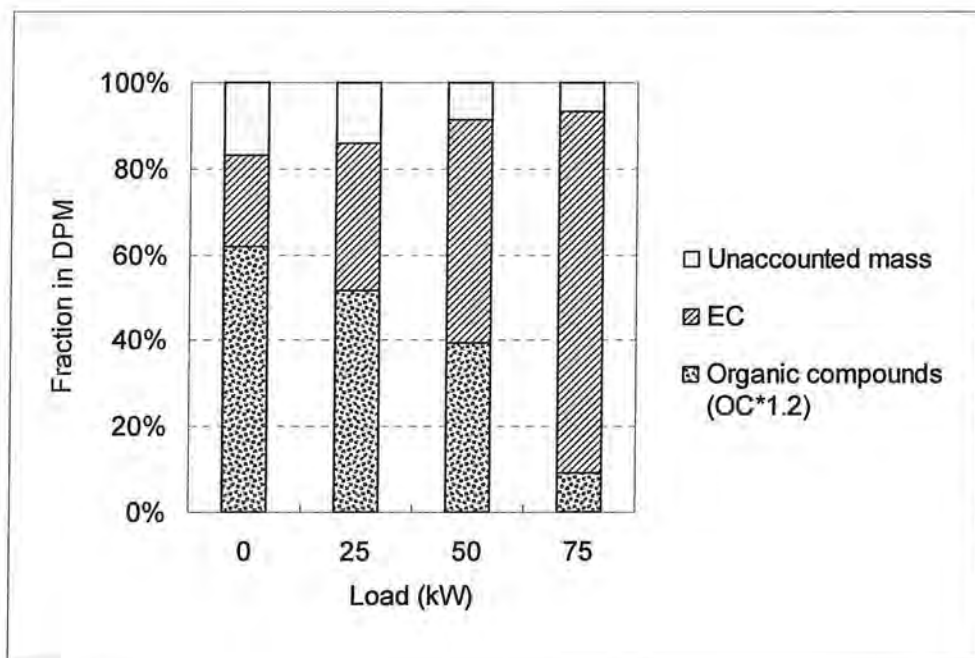


Figure 2-4 Fractions of organic compounds, EC and unaccounted mass in DPM vs. load

(Sulfur content = 500ppm, Collection temperature = 120 ± 14 °C)

In Table 2-1, OC/EC distributions reported by different researchers are listed. Although OC/EC emissions are largely dependent on engine conditions, it still can be found that the CF (total carbonaceous fraction)/DPM ratios reported here are comparable with that in most of other researches. However, most researchers reported relatively higher OC/DPM ratios, which is likely due to their dilution conditions.

Table 2-1 OC/EC distributions reported by different researchers

	EC/DPM	OC/DPM	CF/DPM	Fuel sulfur content	Sampling condition	Dilution ratio
This study	21%-84%	9%-62%	83%-93%	500ppm	Undiluted, Method 5	1
Shah, 2004 (9)	17.3%-67.8%	28.8%-72.7%	90%-96%	<15ppm	Secondary Dilution	
Rogers, 2002 (10)	20±8%	60±30%	89%	380ppm	Dilution	18-20
Kelly, 2003 (2)	2.58%-29.7%	51.6%-75.5%	79.5%		Dilution	31.3-42
Shi, 2000 (1)	24.58%-51.52%	24.46%-57.66%	58.40%-92.24%	427ppm	Dilution	3.7-2221
Cadel, 1999 (5)			88%	#2diesel	Dilution	

2.3.2 Influence of the Sulfur Content in Diesel Fuels

Figure 2-5 and Figure 2-6 present concentrations and fractions of organic compounds, EC, and unaccounted mass in DPM respectively at various loads for the high sulfur diesel (fuel sulfur content at 3700ppm) and a collection temperature of 120 °C \pm 14 °C. The increase of EC fractions and decrease of organic compound fractions with increasing load is consistent with the low sulfur diesel. Consistent with a previous study, more DPM was collected at higher fuel sulfur content (6). However, the organic compounds and the unaccounted mass contribute more to DPM in the high sulfur diesel emissions than in the low sulfur diesel emissions. In the high sulfur diesel emissions, the organic compounds account for 19% to 77% as opposed to 9% to 62% in the low sulfur diesel emissions; and

the unaccounted mass accounts for 18% to 27% as opposed to 7% to 17% in the low sulfur diesel emissions.

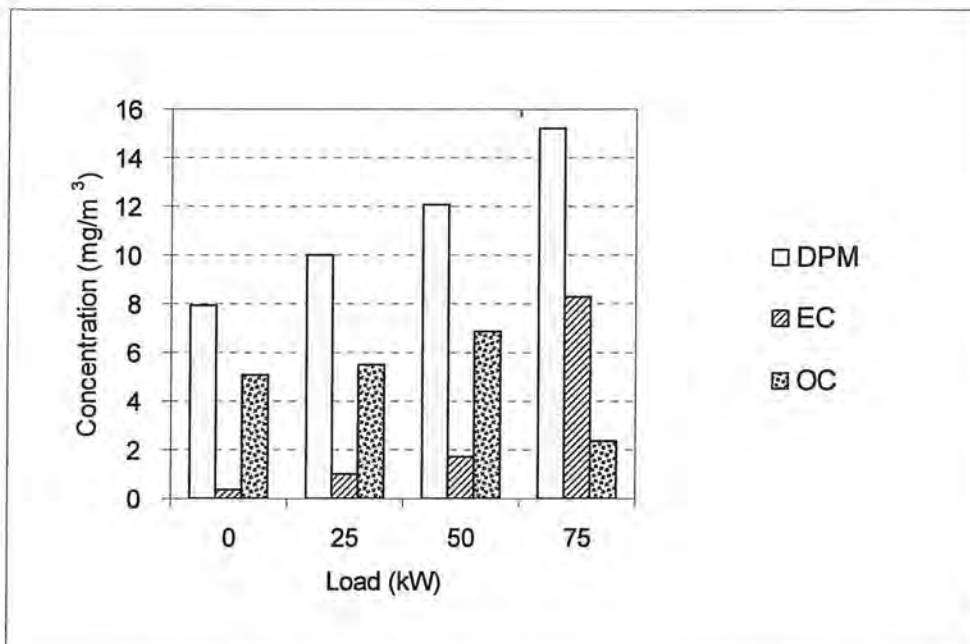


Figure 2-5 Concentration of OC, EC, and DPM vs. engine load
(Sulfur content = 3700ppm, collection temperature = 120 °C ± 14 °C)

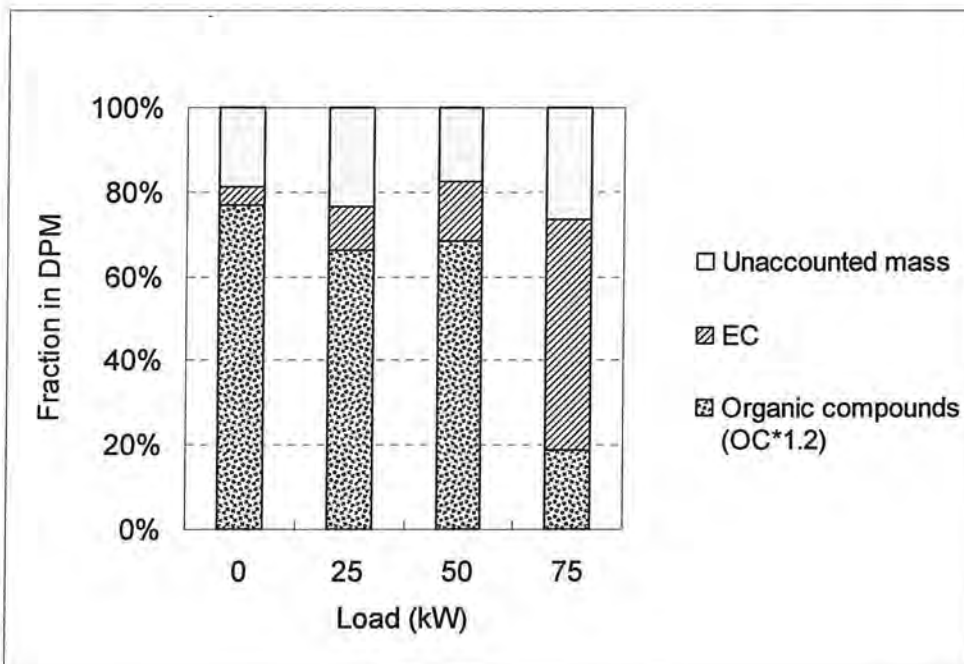


Figure 2-6 Fractions of organic compounds, EC, and unaccounted mass in DPM vs. load

(Sulfur content = 3700ppm, collection temperature = 120 °C ± 14 °C)

As suggested in Figure 2-7, in the high sulfur diesel emissions, the organic compounds measured are 2.5 to 3.6 times higher than in the low sulfur diesel emissions, and the unaccounted mass measured is 3.2 to 6.4 times higher than in the low sulfur diesel emissions. The increase of organic compounds in the high sulfur diesel emissions is consistent with what has been presented by Wall and Hoekman (11), who reported that the soluble organic fraction (SOF) in DPM increases with increasing sulfur content in diesel. The higher sulfur content results in higher concentrations of sulfur acid, which promotes the nucleation of organic compounds (5). The increase of unaccounted mass may partially be the result of the increase of sulfate fractions. Research is underway to study the compositions of the unaccounted mass with load variations.

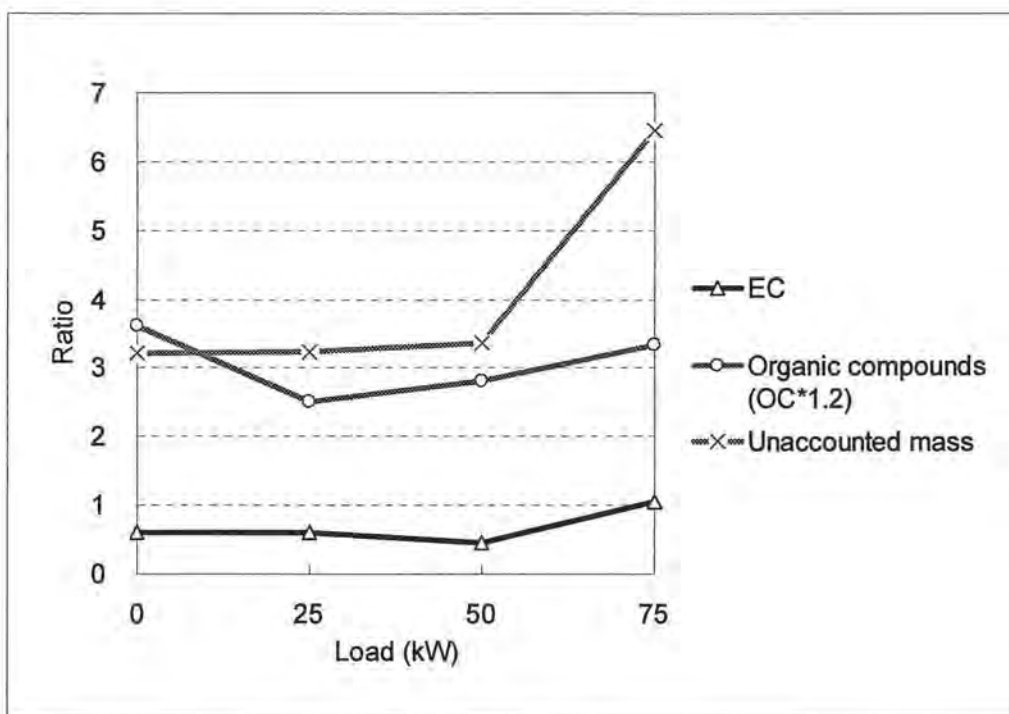


Figure 2-7 Ratios of organic compounds, EC, and unaccounted mass concentrations in the high sulfur diesel (sulfur content = 3700ppm) emissions over those in the low sulfur diesel (sulfur content = 500ppm) emissions

(Collection temperature = 120 °C ± 14 °C for both)

In Figure 2-8, the OC/EC ratios for the high sulfur diesel are compared with those for the low sulfur diesel at various loads. Significantly more OC was obtained from the high sulfur fuel at lower loads, and the OC/EC ratio rapidly decreased with load increase. For the low sulfur diesel, the OC/EC ratios decreased from 2.41 at 0 kW to 0.09 at 75 kW. For the high sulfur diesel, the OC/EC ratios decreased dramatically from 14.71 at 0 kW to 0.29 at 75 kW. The OC/EC ratios are obviously influenced by sulfur content of diesel fuel.

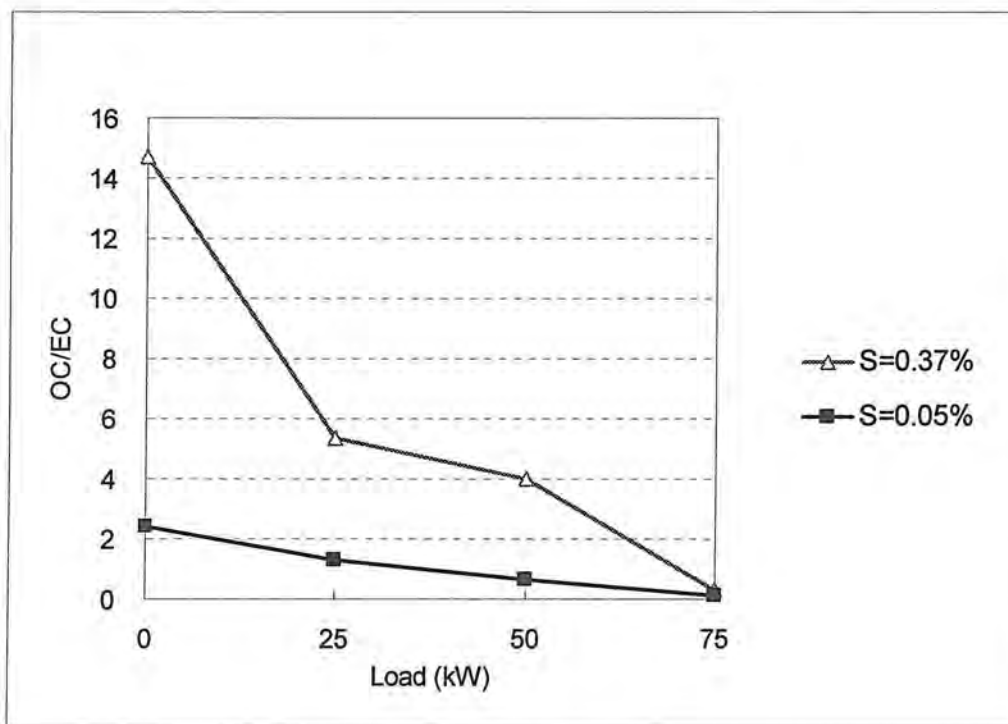


Figure 2-8 OC/EC vs. load

(S = sulfur content, collection temperature = $120\text{ }^{\circ}\text{C} \pm 14\text{ }^{\circ}\text{C}$)

2.3.3 Influence of DPM Collection Temperatures

The fractions of organic compounds, EC, and unaccounted mass in DPM at various loads for the low sulfur diesel (diesel sulfur content = 500ppm) and a collection temperature of $25\text{ }^{\circ}\text{C} \pm 3\text{ }^{\circ}\text{C}$ are shown in Figure 2-9, and their trends with load are consistent with those in Figures 2-4 and 2-6. At the collection temperature of $25\text{ }^{\circ}\text{C} \pm 3\text{ }^{\circ}\text{C}$, the organic

compounds account for 27% to 75% of the DPM mass, as opposed to 9% to 62% at the collection temperature of $120\text{ }^{\circ}\text{C} \pm 14\text{ }^{\circ}\text{C}$.

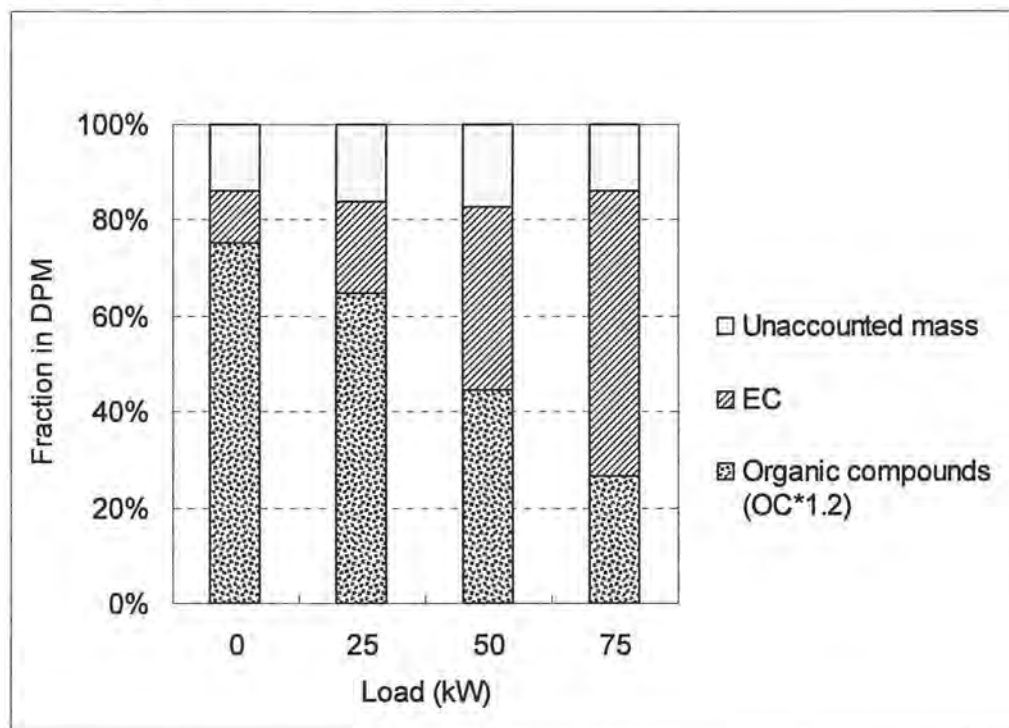


Figure 2-9 Fractions of organic compounds, EC, and unaccounted mass in DPM vs. load (Sulfur content = 500ppm, collection temperature = $25\text{ }^{\circ}\text{C} \pm 3\text{ }^{\circ}\text{C}$)

In Figure 2-10, the ratios of organic compounds, EC, and unaccounted mass concentrations collected at $25\text{ }^{\circ}\text{C} \pm 3\text{ }^{\circ}\text{C}$ and $120\text{ }^{\circ}\text{C} \pm 14\text{ }^{\circ}\text{C}$ are presented. At the collection temperature of $25\text{ }^{\circ}\text{C} \pm 3\text{ }^{\circ}\text{C}$, both organic compounds and unaccounted mass concentrations are much higher than in DPM collected at $120\text{ }^{\circ}\text{C} \pm 14\text{ }^{\circ}\text{C}$, an indication of more condensation of both of these components from vapor to particle phase at lower temperatures. As expected for EC (nonvolatile particulate matter), almost no differences were observed at the two different collection temperatures, which indicates that the EC concentrations were not much influenced by the collection temperature. The decreased OC ratios (OC at $25\text{ }^{\circ}\text{C}$ relative to that at $120\text{ }^{\circ}\text{C}$) at 25 kW and 50 kW are consistent with the findings of Ning *et al.* (11), who reported higher SOFs at low and high loads than at medium load due to increased condensation and nucleation of organic compounds

under low and high load conditions.

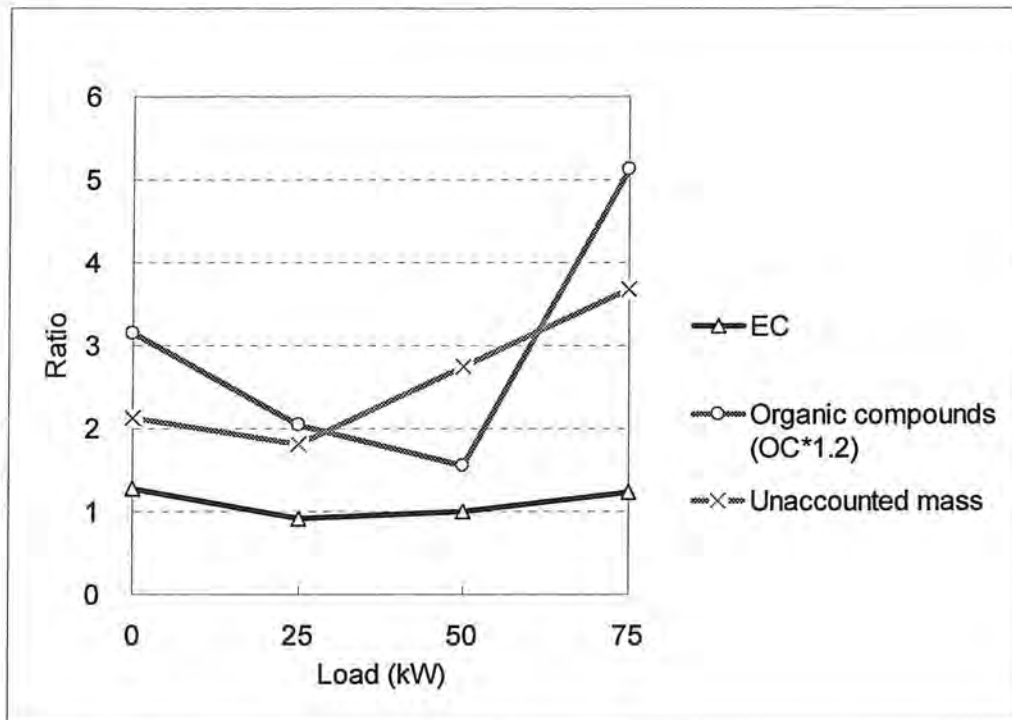


Figure 2-10 Ratios of organic compounds, EC, and unaccounted mass concentrations for a collection temperature of $25\text{ }^{\circ}\text{C} \pm 3\text{ }^{\circ}\text{C}$ over that for a collection temperature of $120\text{ }^{\circ}\text{C} \pm 14\text{ }^{\circ}\text{C}$ (sulfur content = 500ppm)

In Figure 2-11, the OC/EC ratios for a collection temperature of $25\text{ }^{\circ}\text{C} \pm 3\text{ }^{\circ}\text{C}$ are compared with those found at $120\text{ }^{\circ}\text{C} \pm 14\text{ }^{\circ}\text{C}$. At a collection temperature of $25\text{ }^{\circ}\text{C} \pm 3\text{ }^{\circ}\text{C}$, the OC/EC ratios decrease from 5.95 at 0 kW to 0.37 at 75 kW. The OC/EC ratios at $25\text{ }^{\circ}\text{C} \pm 3\text{ }^{\circ}\text{C}$ are 2.5 to 4.1 times higher than those obtained at $120\text{ }^{\circ}\text{C} \pm 14\text{ }^{\circ}\text{C}$. The higher OC fractions found at the lower temperature reflect the collection of a larger amount of condensable organic compounds (semi-volatile fraction) at lower temperature.

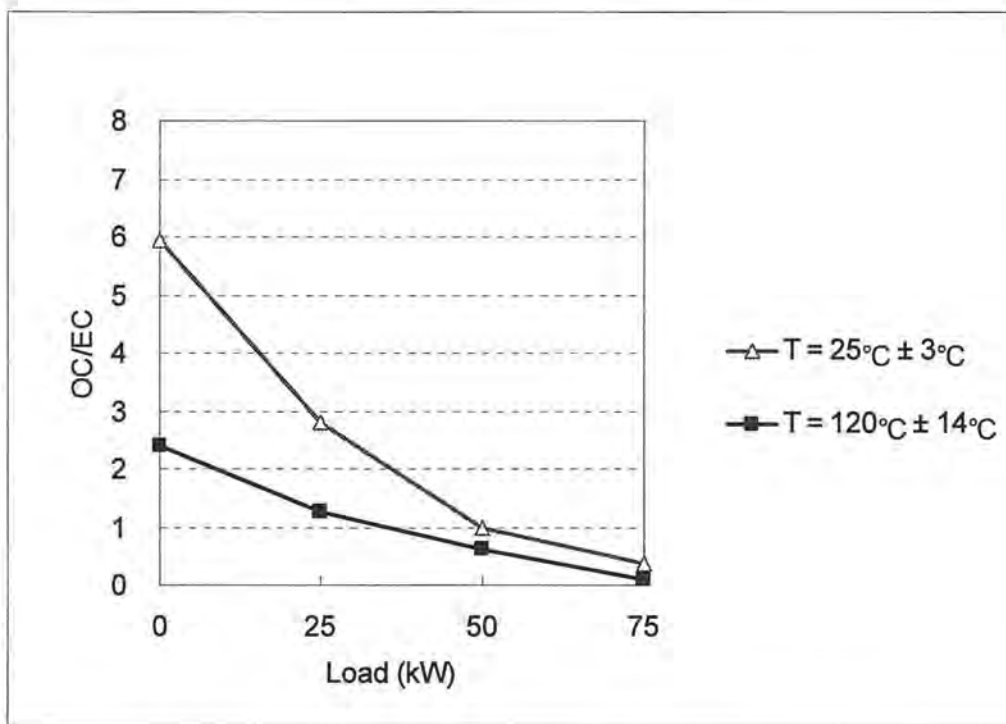


Figure 2-11 OC/EC vs. load (Sulfur content = 500ppm, T = temperature)

2.4 Conclusions

DPM concentrations and the relative contributions of OC, EC, and unaccounted mass vary greatly with engine load, fuel sulfur content, and sample collection temperature.

Specifically, the following results were obtained in this study:

- The EC concentrations in DPM exhaust increase with increasing load, while the OC concentrations do not show great variation with load. The fraction of EC increases with increasing load, while that of OC decreases. The same trends exist regardless of the sulfur content and DPM collection temperature.
- Both the organic compounds and non-carbonaceous materials (unaccounted mass) contribute more to DPM in the high sulfur diesel emissions than in the low sulfur diesel emissions. The OC/EC ratios are higher in the high sulfur diesel emissions than in the low sulfur diesel emissions.

- Both the organic compounds and unaccounted mass concentrations in DPM are significantly influenced by the collection temperature. At lower collection temperatures, more condensation of these components occurs. Thus, the collection temperature has a great influence on the OC/EC ratios.

Previous studies on the OC/EC variation with load conditions for new, heavy duty diesel vehicles have been reported, but relatively little information is available for non-road diesel generators. Studies on these types of engines are important because DPM emissions from non-road diesel engines are significantly higher than those from on-road sources. The findings of this study may prove useful to the control and regulation of non-road diesel generators in this capacity range. A paper entitled "Variation in the Particulate Carbon Distribution from a Non-road Diesel Generator" as a result of this study has been accepted to *Environ. Sci. Technol.* 2005.

2.5 References

- (1) Shi, J.P.; Mark, D.; Harrison, R.M. Characterization of particles from a current technology heavy-duty diesel engine. *Environ. Sci. Technol.* 2000, Vol. 34, No. 5, 748-755.
- (2) Kelly, K.E.; Wagner, D.A.; Lighty, J.S.; Sarofim, A.F. Characterization of exhaust particles from military vehicles fueled with diesel, gasoline, and JP-8. *J. Air & Waste Manage. Assoc.* 2003, Vol. 53, No. 3, 273-282.
- (3) Federal Register, Part II, Environmental Protection Agency. Amendments for testing and monitoring provisions. Final Rule, 40 CFR Part 60, 61, and 63; Tuesday, October 17, 2000. See <http://www.epa.gov/ttn/emc/promgate.html> for method details.
- (4) Cassinelli, M.E., O'Connor, P.F., eds. NIOSH manual of analytical methods (NMAM). Second supplement to NMAM; U.S. Department of Health and Human Services (DHHS), Public Health Service, Centers for Disease Control, National Institute for Occupational Safety and Health (NIOSH). 4th Edition. Publication No. 94-113. Cincinnati, OH. 1998.

- (5) Cadle, S.H.; Nelson, K.; Ragazzi, R.A.; Barrett, R.; Gallagher, G.L.; Lawson, D.R.; Knapp, K.T.; Snow, R. Composition of Light-Duty Motor Vehicle Exhaust Particulate Matter in the Denver, *Environ. Sci. Technol.* V1999, 33(14), 2328-2339.
- (6) Saiyasitpanich, P.; Lu, M.; Keener, T.C.; Khang, S.J.; Liang, F. The effect of diesel fuel sulfur content on particulate matter emissions for a nonroad diesel generator. *J. Air & Waste Manage. Assoc.*, in press.
- (7) Gray, H.A.; Cass, G.R.; Huntzicker, J.J.; Heyerdahl, E.K.; Rau, J.A. Characteristics of atmospheric organic and elemental carbon particle concentrations in Los Angeles. *Environ. Sci. Technol.* 1986, Vol. 20, 580-582.
- (8) Burtcher, H.; Kunzel, S.; Hüglin, C. Characterization of particles in combustion engine exhaust. *J. Aerosol Sci.* 1998, Vol. 29, No.4, 389-396.
- (9) Shah, S.D.; Cocker, D.R.; Miller, J.W. Norbeck, J.M. Emission rates of particulate matter and elemental and organic carbon from in-use diesel engines. *Environ. Sci. Technol.* 2004, 38, 2544-2550.
- (10) Rogers, F.C.; Sagebiel, J.C.; Zielinska, B.; Arnott, P.W.; Fujita E.M.; McDonald, J.D.; Griffin, J.B.; Kelly, K.E.; Overacker, D.; Wagner, D.; Lighty, J.S.; Sarofim, A.; Palmer, G. Characterization of submicron exhaust particles from engines operating without load on diesel and JP-8 fuel. *Aerosol Sci. Tech.* 2003, Vol. 37, 355-368.
- (11) Wall, J.C., Hoekman, S.K. Fuel composition effects on heavy-duty diesel particulate emissions. SAE Technical Paper Series, 841364, Fuel and Lubricant Meeting & Exposition, Baltimore, Maryland, October 8-11, 1984.
- (12) Shi, J.P.; Harrison, R.M. Investigation of ultrafine particle formation during diesel exhaust dilution. *Environ. Sci. Technol.* 1999, Vol. 33, 3730-3736.
- (13) Ning, Z.; Cheung, C.S.; Liu, S.X. Experimental investigation of the effect of exhaust gas cooling on diesel particulate. *J. Aerosol Sci.* 2004, Vol. 35, 333-345.

Chapter 3 Investigation of Sulfur Species Distribution in Non-road Diesel Emissions

3.1 Introduction

Various sulfur species exist in non-road diesel emissions in gaseous and particulate phases. Sulfur dioxide (SO_2) is a priority air pollutant regulated under the National Ambient Air Quality Standards, and sulfate (SO_4^{2-}) is supposed to play an important role in fine particulate formation and the nucleation of organic compounds (1). This study investigated the variations of sulfur speciation in non-road diesel emissions. The objective of this study was to provide a detailed account of the sulfur compound distributions for a diesel generator under various load conditions and to obtain a sulfur balance going in and out of the generator. The correlations between the sulfur content in diesel and the distribution of sulfur species in diesel emissions were established. As a result of this study, the sensitivity of sulfur species to fuel sulfur level under various engine load conditions has been determined.

3.2 Experimental methods

Tests were performed on a Generac diesel generator rated at 80 kW and 1800 rpm. A load simulator (model Merlin 100 by Simplex) was used to simulate various load conditions from 0 kW to 75 kW. EPA Method 8 (Determination of Sulfuric Acid and Sulfur Dioxide Emissions from Stationary Sources) (2) was utilized. DPM samples were collected on Teflon filters at the same time as measuring sulfur dioxide (SO_2) and sulfuric acid (H_2SO_4) in emissions.

In EPA Method 8, the undiluted exhaust is sampled through a heated sampling probe. SO_2 and H_2SO_4 are collected and measured separately by the barium-thorin titration method. One impinger containing isopropanol (80%) is used to absorb H_2SO_4 . Two impingers that follow containing H_2O_2 (3%) are used to absorb SO_2 . DPM was collected by inserting a heated ($120 \pm 14^\circ\text{C}$) Teflon filter (Pall Gelman, $1.0\mu\text{m}$) between the probe

and isopropanol impinger.

Particulate sulfate (SO_4^{2-}) was determined by Ion Chromatography (IC) analysis of the DPM samples. Samples were submerged in 25.0 ml deionized water and extracted with ultrasonic shaking for 60 min. A Dionex 500 ion chromatography was employed for IC measurement. It was found that adding ethanol can improve the extraction efficiency of SO_4^{2-} from Teflon filter. However, ethanol can disturb the pressure of ion chromatography column. So it needs to be removed from the sample before the sample is injected into the ion chromatography column.

Total particulate sulfur was determined by X-Ray Fluorescence (XRF) spectroscopy analysis of the DPM samples by a commercial source (CHESTER LabNet). EPA Method IO-3.3 [Determination of Metals in Ambient Particulate Matter Using X-Ray Fluorescence (XRF) Spectroscopy] was employed.

High and low sulfur #2 diesel fuels were used in this study to evaluate the potential influence of fuel sulfur content on the sulfur species distribution. The low sulfur diesels have a light color and their sulfur contents are 300ppm, 400ppm and 450ppm by weight. The high sulfur diesels have a red color and their sulfur contents are 1300ppm, 1750ppm and 2200ppm by weight. Sulfur content in diesel fuel was determined by a commercial source (OKI lab) and confirmed by AED analysis.

3.3 Results and discussions

3.3.1 SO_2

(1) Measured SO_2 concentration

In all the sulfur species, Sulfur dioxide is the one that have most clear relationship with both load and diesel sulfur content. Figure 3-1 shows that SO_2 concentration is clearly related to diesel sulfur content as well as engine load conditions in non-road diesel emissions. SO_2 concentration increases as diesel sulfur content or engine load increase. In

this study, diesel fuels with six different sulfur contents were used.

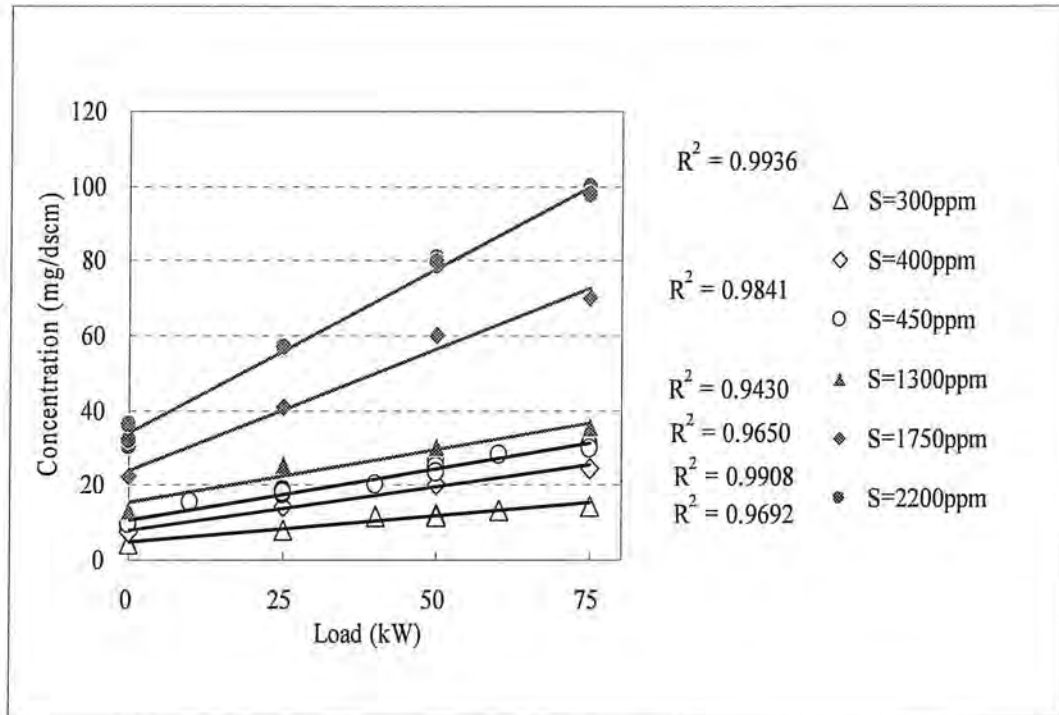


Figure 3-1 SO₂ concentrations

Based on the diesel sulfur content and diesel consumption rate, the total consumed sulfur can be calculated. Comparing the detected sulfur that in the form of SO₂ with the total consumed sulfur, the diesel sulfur to SO₂ conversion rates can be obtained. The rates will give us an idea how much diesel sulfur converted into SO₂.

Figure 3-2 presents the percent S → SO₂ conversion rate under various loads. As shown in Figure 3-2, the SO₂ conversion rates are obviously related with diesel types. The three high sulfur diesels (red color diesel) have obviously lower conversion rates than the three low sulfur diesels (light color diesel). However, for both the low sulfur diesel and the high sulfur diesel, the conversion rates increase as diesel sulfur content increase.

Analysis of diesel fuels indicated that, the sulfur compounds in the three red high diesel

fuels were obviously different with that in the three light color low sulfur diesel fuels, and they have quite different molecular weight. It was shown that the SO₂ conversion rates are related to both the fuel sulfur level and the forms of sulfur compounds in diesel fuel.

The S → SO₂ conversion rates are from 50% to 100%. It is also found that the SO₂ conversion rates slightly decrease with load.

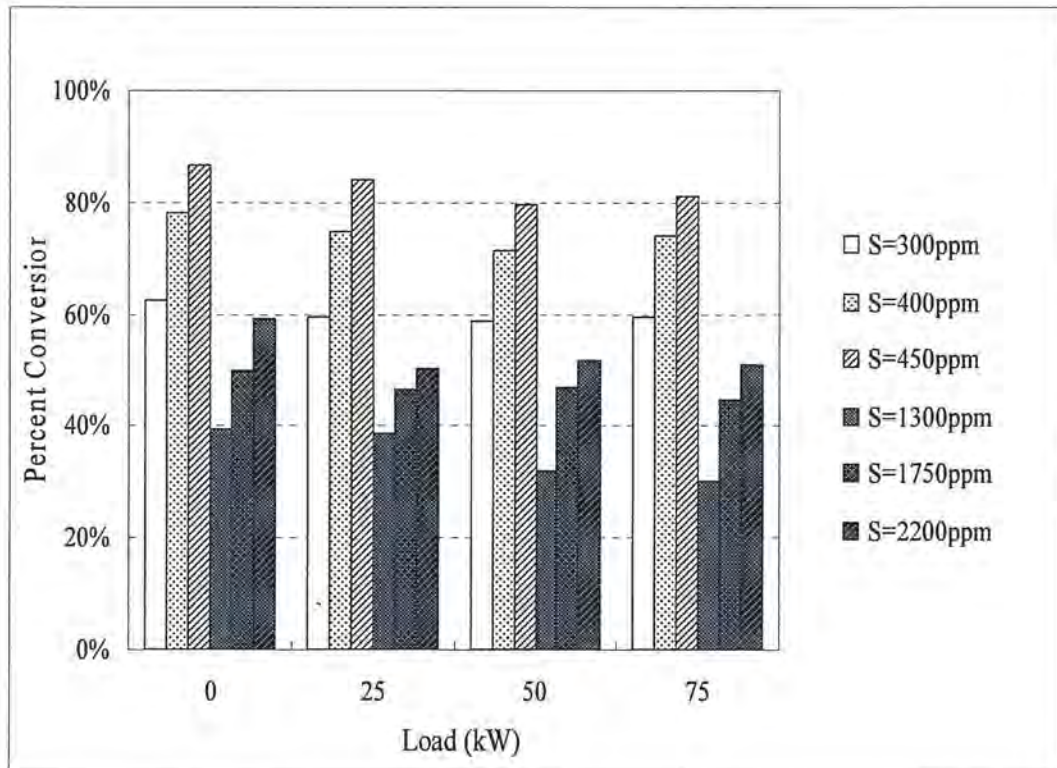


Figure 3-2 S to SO₂ conversion rates

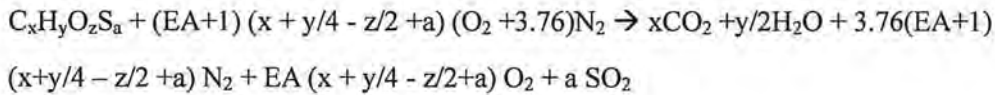
(2) Theoretical SO₂ concentration

Theoretical SO₂ concentration can be calculated based on the diesel compounds analysis results, excess air, and the combustion equation. According to diesel compounds analysis results, mass percent of each element are as following:

$$\begin{aligned} \text{C: } 85\% & \quad 85/12=7.08 \quad 7.08/7.08=1 \\ \text{H: } 14\% & \quad 14/1=14 \quad 14/7.08=1.98 \\ \text{O: } 1\% & \quad 1/16=0.06 \quad 0.06/7.08=0.008 \\ \text{S: } s\% & \quad s/32/7.08=s/226 \end{aligned}$$

So, formula of diesel can be written as $C_xH_yO_zS_a$, in which,
 $x=1, y=1.98, z=0.008, a=s/226$, in which $s\%$ is the diesel sulfur content.

Therefore the combustion equation can be written as:



In which, EA is excess air. Assuming all sulfur in diesel will convert to SO_2 , the SO_2 concentration can be calculated using the following equation:

$$\begin{aligned} C_{(SO_2)} &= a / [x+y/2 + 3.76(EA+1) (x+y/4 - z/2 + a) + EA (x + y/4 - z/2+a) + a] \\ &= s / [786.7 + 1603.9 EA + 4.76 EA*s + 2s] \end{aligned}$$

The calculated theoretical SO_2 concentration and the measured SO_2 concentration are shown in Table 3-1. The ratios of the measured SO_2 concentration over theoretical SO_2 concentration were very close to the S to SO_2 conversion rates in Figure 3-2.

Table 3-1 Comparison of the theoretical and the measured SO_2 concentration

Diesel sulfur content	Load	Theoretical SO_2 Conc.		Measured SO_2 Conc.	Measured SO_2 Conc./ Theoretical SO_2 Conc.	S to SO_2 conversion rates
		(ppm)	(mg/dscm)	(mg/dscm)		
300ppm	0kW	3.07	8.77	4.43	50.5%	62.5%
	25kW	5.86	16.75	8.15	48.7%	59.6%
	50kW	7.66	21.90	12.03	54.9%	58.8%
	75kW	9.64	27.54	14.49	52.6%	59.3%
400ppm	0kW	4.09	11.70	7.25	62.0%	78.0%

	25kW	7.82	22.33	14.47	64.8%	74.8%
	50kW	10.22	29.19	20.19	69.2%	71.4%
	75kW	12.85	36.72	24.52	66.8%	73.9%
450ppm	0kW	4.61	13.16	9.58	72.8%	86.5%
	25kW	8.79	25.12	17.92	71.3%	84.0%
	50kW	11.49	32.84	25.03	76.2%	79.6%
	75kW	14.46	41.30	30.79	74.5%	80.9%
2200ppm	0kW	22.51	64.31	32.04	49.8%	59.1%
	25kW	42.96	122.76	56.71	46.2%	50.3%
	50kW	56.17	160.48	79.48	49.5%	51.8%
	75kW	70.64	201.83	97.80	48.5%	50.8%

3.3.2 SO₄²⁻

The total SO₄²⁻ species include the vapor phase H₂SO₄ which is determined by Method 8, and the particulate SO₄²⁻ which is determined by IC analysis of DPM samples. Figure 3-3 presents the total SO₄²⁻ concentrations in emissions under various loads. It is found that the total SO₄²⁻ concentration is not sensitive with diesel sulfur content. Diesel fuels with different sulfur contents have similar sulfate concentration. We also notice that, it shows a “U” type trend along with load. At high and low loads, there is more SO₄²⁻ than at middle loads.

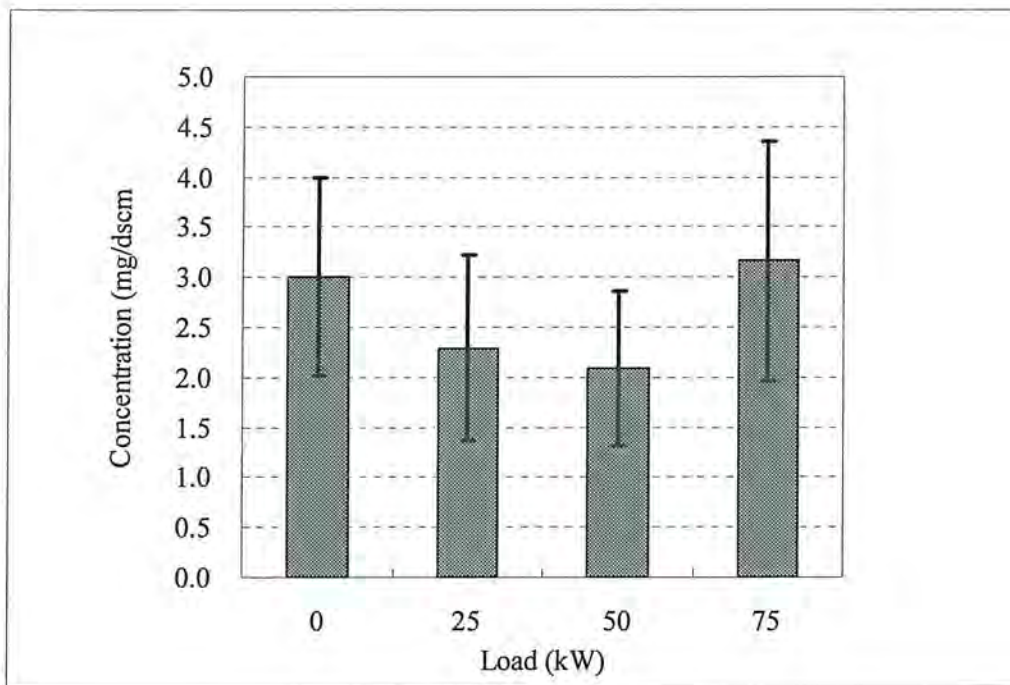


Figure 3-3 Total SO_4^{2-} concentrations

Figure 3-4 presents the percent $\text{S} \rightarrow \text{SO}_4^{2-}$ conversion rate under various loads. It is apparent that high sulfur diesel has lower percent $\text{S} \rightarrow \text{SO}_4^{2-}$ conversion rates than low sulfur diesel. This is consistent with studies by Truex, *et al.* (3), which indicated that diesel SO_4^{2-} formation is not controlled by thermodynamic equilibrium, but must be kinetically limited. Some researchers reported that for small additions of sulfur to the fuel, there is an increase in the sulfates, reaching a maximum and then decreasing to a stable final value (4). Figure 3-4 shows that the conversion rate is much higher at 0kW than that at other loads. Shi, *et al.* (5) reported that the SO_4^{2-} fractions in DPM decreases with decreasing engine load, which is consistent with our results. However, Wall and Hoekman (6) reported that, the conversion rates were insensitive to fuel sulfur level, and at idle the rate was somewhat lower.

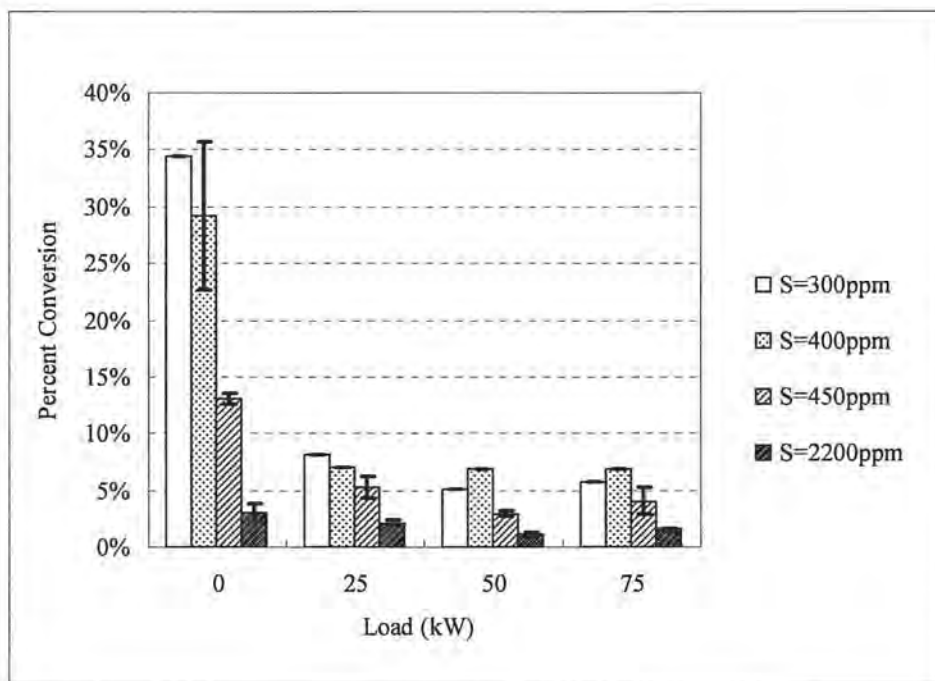


Figure 3-4 S \rightarrow SO₄²⁻ conversion rates

Sulfur consumption increases with load as show in Figure 3-4, and the percent S \rightarrow SO₄²⁻ conversion rates decrease with load as show in Figure 3-5. The combination of these two trends may explain the “U” type trend of SO₄²⁻ concentrations in Figure 3-3. In Chapter 2, Figure 2-10 has shown that at low and high load conditions, there were more soluble organic fractions (SOF) of DPM nucleating and condensing than at medium load conditions. Ning *et al.* (7) also reported the same phenomenon. Since sulfate (SO₄²⁻) is supposed to play an important role in fine particulate formation and the nucleation of organic compounds (1), the “U” type trend of condensed organic compounds may be associated with the “U” type trend of SO₄²⁻ concentrations. This coincidence confirmed the function of sulfate during the condensing of organic compounds.

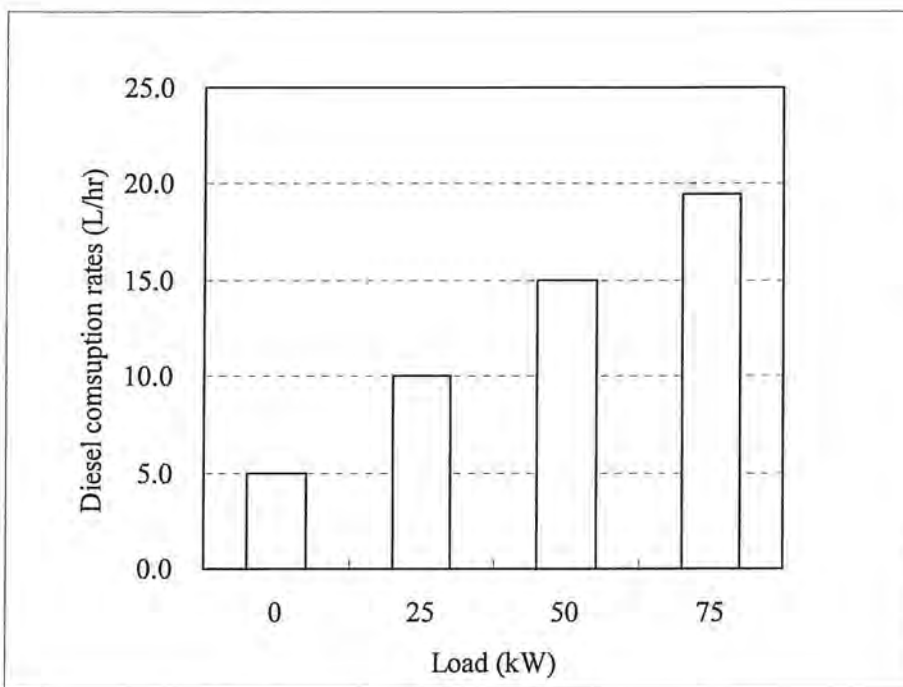


Figure 3-5 Diesel consumption rates

As is well known excess air decreases with engine load. This may explain why the percent $S \rightarrow SO_4^{2-}$ conversion rate decrease with load. The percent $S \rightarrow SO_4^{2-}$ conversion rate vs. excess air is plotted in Figure 3-6. It indicates that the percent $S \rightarrow SO_4^{2-}$ conversion rate is linearly related with excess air as this is an oxidation process.

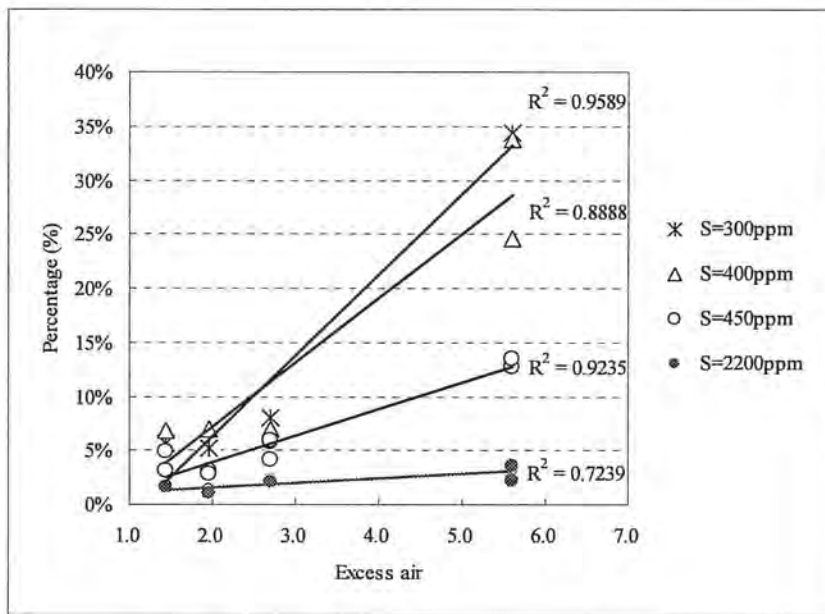


Figure 3-6 S to SO₄²⁻ conversion rate vs. excess air

Figure 3-7 shows that H₂SO₄ occupies 90.5% to 99.2% of the total SO₄²⁻ species present in diesel exhaust. The results are comparable with what has been reported by Truex, *et al.* (3). The highest percentages were achieved at 0kW load.

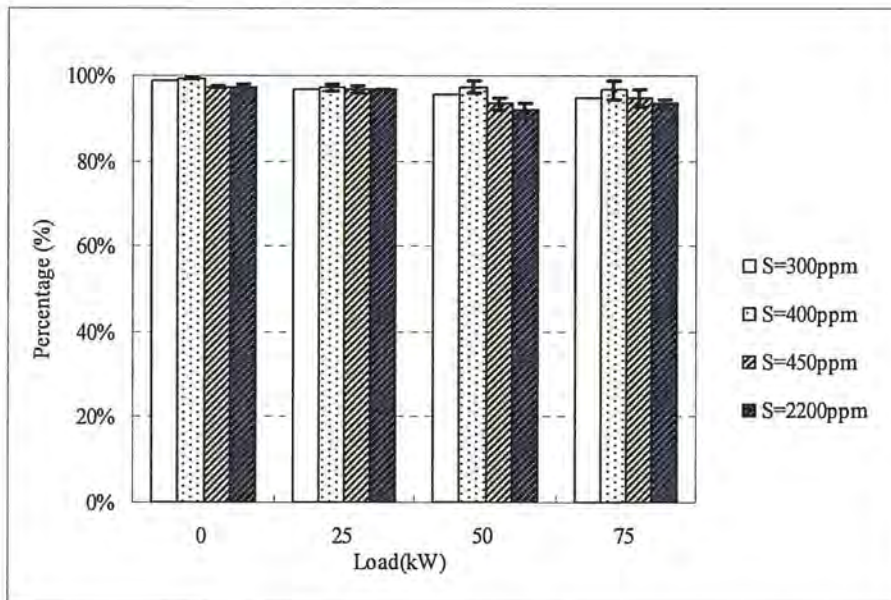


Figure 3-7 Vapor phase SO₄²⁻ / Total SO₄²⁻

3.3.3 Particulate Sulfur

Figure 3-8 presents the total particulate sulfur concentrations in emissions under various loads, and Figure 3-9 presents the percent of S conversion to total particulate sulfur (TPS) conversion rates. It indicates that the TPS concentration increases as diesel sulfur content or engine load increase. The percent S→TPS conversion rates range from 0.12% to 0.50%, and decrease as diesel sulfur content increases. The rates do not seem to be strongly correlated with engine load.

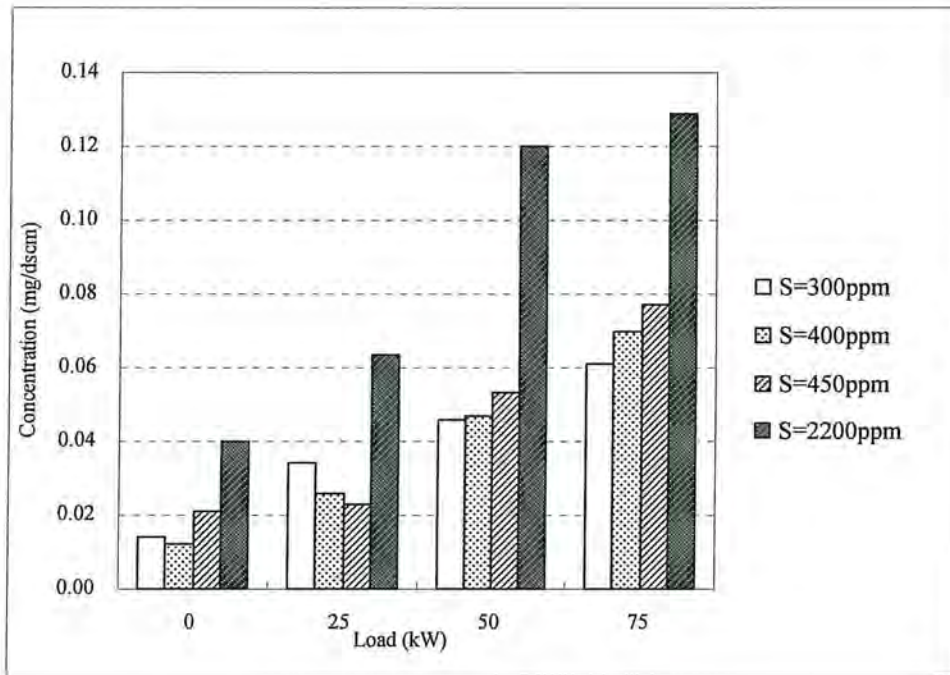


Figure 3-8 Total particulate sulfur concentrations

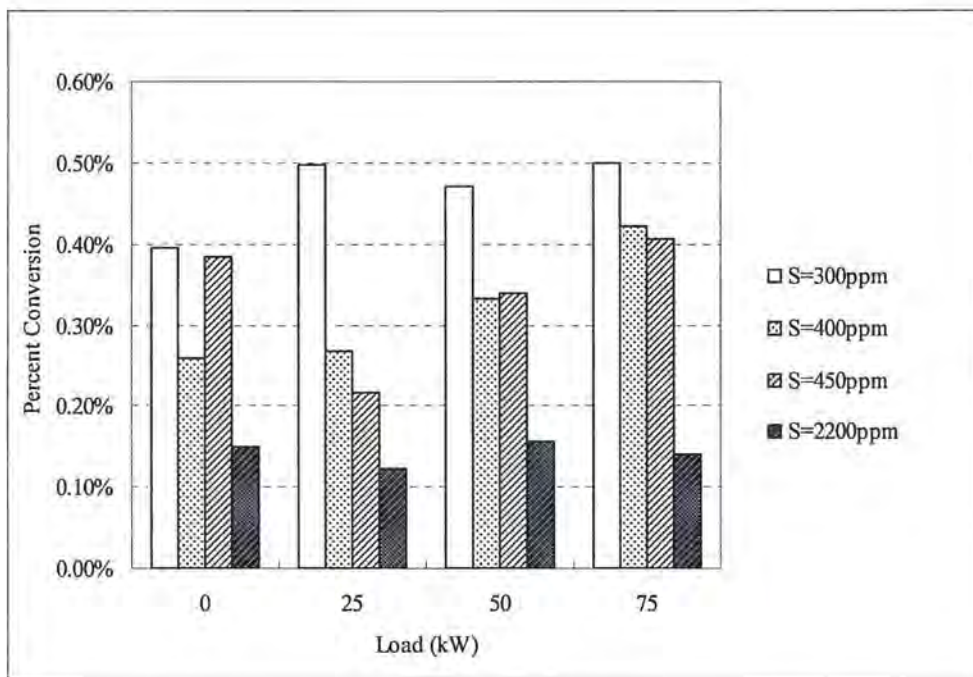


Figure 3-9 S to total particulate sulfur (TPS) conversion rates

Figure 3-10 presents the Particulate Sulfate-S/TPS ratio under various loads. It shows how much total particulate sulfur are in the form of sulfate. At 0kW load, the ratio is very sensitive to diesel types. For high sulfur diesel, Particulate Sulfate occupies only 50% of Total Particulate Sulfur, while for low sulfur diesel it may occupy as high as 100% of Total Particulate Sulfur. But at high load, different diesels have similar Particulate Sulfate to Total Particulate Sulfur ratios, of about 60%. Cadle (8) reported that IC sulfate measurement is well correlated with the total sulfur measured by X-ray fluorescence (XRF), with ratios from 0.4 to 0.5. This is consistent with our studies at high loads. However, at low loads (0kW and 25kW), the ratio is very sensitive to fuel sulfur contents.

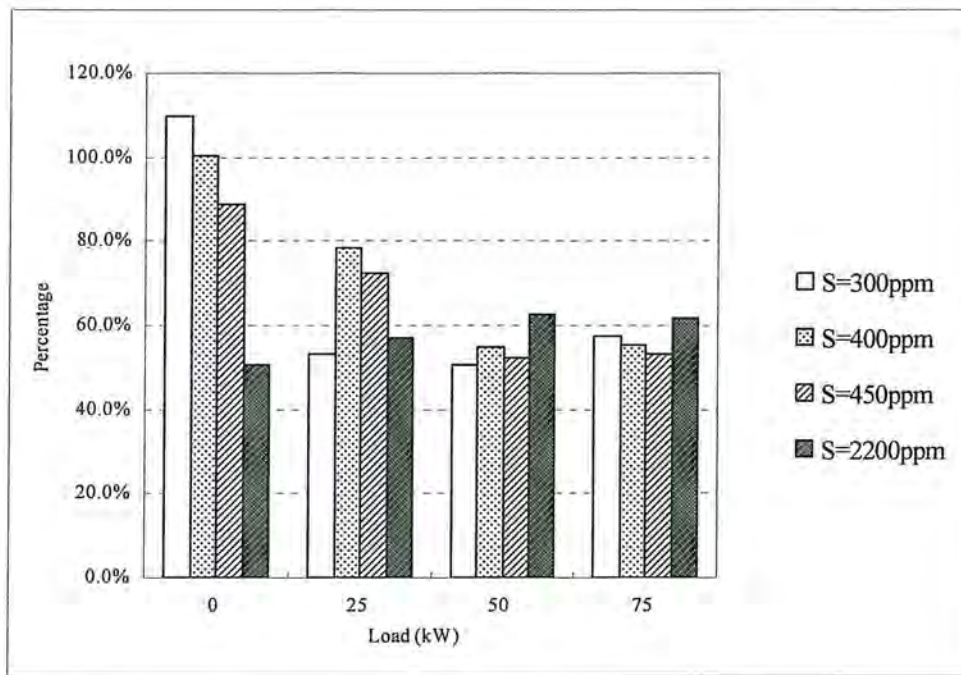


Figure 3-10 Particulate Sulfate-S/TPS ratio under various loads

3.3.4 The Balance of Sulfur Input and Output

Figure 3-11 gives the balance/recovery of sulfur input and output for different diesel fuels under various loads. The highest sulfur recoveries were achieved at 0kW load for all the diesel fuels. It can be as high as 100%. At higher loads, the air to fuel ratio is lower, so there may be some sulfur not oxidized in emissions, such as organic sulfur compounds, hydrogen sulfide (H_2S), carbonyl sulfide (OCS), etc. Though not measured in our study, these species have been identified in other studies with diesel and gasoline vehicles. Maricq (9) reported that the sulfur emissions are primarily in the form of SO_2 , with a minor component of H_2S in gasoline emissions. Although diesel exhaust is more oxidizing than a typical exhaust from gasoline engines(10), Braddock *et al.* (11), Perez (12), Cadle (13), Fried *et al.* (14) have reported that H_2S or OSC has been detected in emissions of diesel fuel vehicles. Since we mainly measured oxidized form of sulfur, these sulfur compounds are not detected in our study, so the sulfur recovery is lower at higher loads.

The sulfur recovery is also sensitive to diesel types. This may indicate that some types of diesel fuels have more sulfur not oxidized in their emissions. The red high sulfur diesel has obviously lower sulfur recovery than the other three light color low sulfur diesel fuels. It is found that, the sulfur compounds in the red high sulfur diesel were obviously different with that in other three light color low sulfur diesel fuels, and they have quite different molecular weight. The sulfur recovery may be related to the forms of sulfur compounds in diesel fuels.

Further investigation on reduced sulfur or other vapor phase sulfur compounds in diesel emissions is needed.

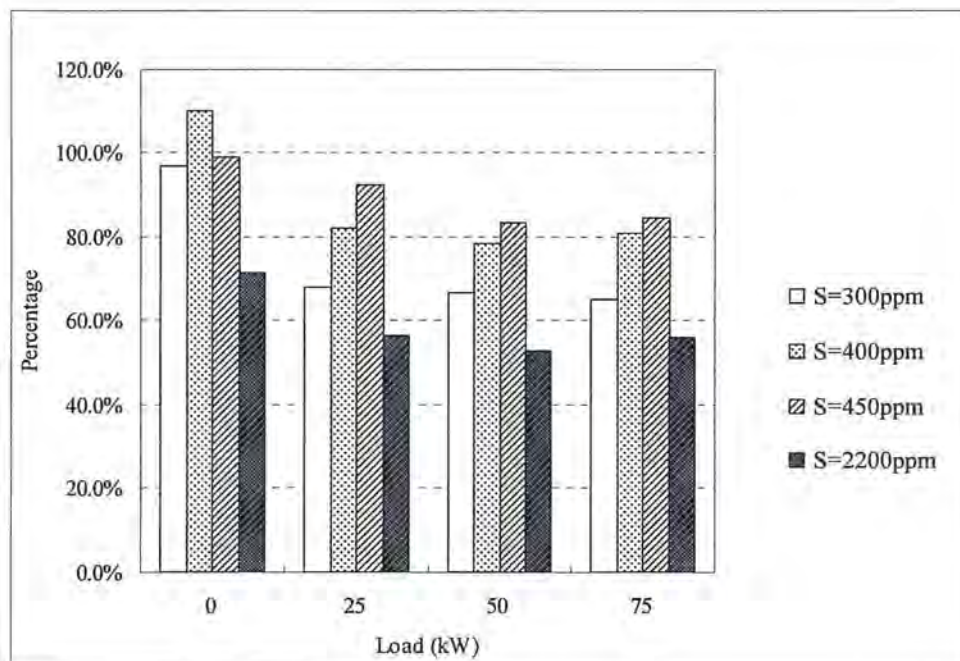


Figure 3-11 Sulfur recovery

3.4 Conclusions

The distributions of various sulfur species are closely related with engine load and fuel sulfur content. The major conclusions obtained in this study include:

- SO₂ concentration is clearly related to diesel sulfur content as well as engine load conditions in non-road diesel emissions. The S→SO₂ conversion rates slightly decrease with increasing load. And they are obviously related with diesel types. For the same type of diesel, the conversion rates increase as diesel sulfur content increase.
- The total SO₄²⁻ concentration is not sensitive to diesel sulfur content and they show a “U” type trend for increases in load. The percent S→SO₄²⁻ conversion rates decreases with fuel sulfur content. The percent S→SO₄²⁻ conversion rate decreases as engine load increases and is linearly related to excess air. More than 90% of the total sulfates are in the form of H₂SO₄.
- The TPS concentration increases as diesel sulfur content or engine load increases. The percent S→ TPS conversion rates are from 0.12% to 0.50%, and decrease as diesel sulfur content increases. The Particulate Sulfate-S/TPS ratios are from 50% to 100%. The ratio is more affected by the fuel sulfur content at lower loads, and tend be consistent at high loads. The sulfur recovery is sensitive to diesel fuel types and may be related to the forms of sulfur compounds in diesel fuel.

A paper entitled “The Sulfur Speciation of Diesel Emissions from a Non-road Generator” as a result of this study has been submitted to the Air and Waste Management Association (A&WMA) 97th Annual Conference & Exhibition, Minneapolis, 2005.

3.5 References

- (1) Shi, J.P.; Harrison, R.M. Investigation of Ultrafine Particle Formation during Diesel Exhaust Dilution, *Environ. Sci. Technol.* 1999, Vol. 33, 3730-3736
- (2) *Amendments for Testing and Monitoring Provisions; Final Rule.* Federal Register,

Part II, 40 CFR Part 60, 61, and 63; U.S. Environmental Protection Agency; Tuesday, October 17, 2000. See <http://www.epa.gov/ttn/emc/promgate/m-08.pdf> for method details (accessed March 2005).

- (3) Truex, T.J.; Pierson, W.R.; McKee, D.E. Sulfate in Diesel Exhaust, *Environ. Sci. Technol.* Vol. 14, September 1980, Number 9, 1118-1121.
- (4) Lucasa, A.; Dura'n, A.; Carmona, M.; Lapuerta, M. Modeling Diesel Particulate Emissions with Neural Networks, *Fuel*, 2001, 80, 539-548.
- (5) Shi, J.P.; Mark, D.; Harrison, R.M. Characterization of Particles from a Current Technology Heavy-Duty Diesel Engine, *Environ. Sci. Technol.* 2000, 34, 748-755.
- (6) Wall, J.C.; Hoekman, S.K. Fuel Composition Effects on Heavy-Duty Diesel Particulate Emissions, *SAE Technical Paper Series*, 841364; Fuel and Lubricant Meeting&Exposition, Baltimore, Maryland. October 8-11, 1984.
- (7) Ning, Z.; Cheung, C.S.; Liu, S.X. Experimental Investigation of the Effect of Exhaust Gas Cooling on Diesel Particulate, *Journal of Aerosol Science*. 2004, Vol. 35, 333-345.
- (8) Cadle, S.H.; Mulawa, P.A.; Hunsanger, E.C. Composition of Light-Duty Motor Vehicle Exhaust Particulate Matter in the Denver, *Environ. Sci. Technol.* 1999, Vol 33, No.14, 2328-2339.
- (9) Maricq, M.M.; Chase, R.E.; Xu, N.; Podsiadlik, D.H. The Effects of the Catalytic Converter and Fuel Sulfue Level on Motor Vehicle Particulate Matter Emissions: Gasoline Vehicles, *Environ. Sci. Technol.* 2002, Vol 36, No.2, 276-282.
- (10) Corro, G. Sulfur Impact on Diesel Emission Control - A Review, *React.Kinet.Catal.Lett.* Vol. 75, No. 1, 89-106, 2002
- (11) Braddock, J.N.; Gabele, P.A. Emission Patterns of Diesel-Powered Passenger Cars - Part II. *SAE Prepr.* Feb 28--Mar 4, 1977, n 770168.
- (12) Perez, J.M. Measurement of Unregulated Emissions: Some Heavy Duty Diesel Engine Results, *Environment International*. 1981, v 5, n 4-6. p 217-228.
- (13) Cadle, S.H.; Nebel, G.J.; Williams, R.L. Measurement of Unregulated Emissions from General Motors' Light-Duty Vehicles, *SAE Prepr.* 1979, n 790694.
- (14) Fried, A.; Henry, B.; Ragazzi, R.; Merrick, M.; Stokes, J.; Pyzdrowski, T.; Sams, R.

Measurement of Carbonyl Sulfide in Automotive Emissions and an Assessment of Its Importance to the Global Sulfur Cycle, *Journal of Geophysical Research-Atmospheres*, Sep 20, 1992, 97 (D13): 14621-14634.

Chapter 4 Investigation of Organic DPM Sampling Artifacts of a High-volume Sampling System

4.1 Introduction

4.1.1 Sampling artifacts of organic aerosol

A common method for measuring the mass of organic aerosol involves filter collection and subsequent thermal analysis. Quartz fiber filters are often used because they are suitable for thermal analysis which heats samples as high as 800°C and quartz fiber filters can be easily extracted (1). However, quartz fiber filters have a large specific surface area upon which adsorption of gases can be great. If unaccounted for, the adsorption of organic vapors onto the filter during and/or after sample collection will lead to the overestimation of organic aerosol concentrations and comprises positive artifacts.

On the other hand, volatilization of organic aerosol can occur if a significant pressure drop develops across the filter. Due to pressure gradient that exists through a filter, particles deep within the filter will be exposed to gas-phase concentrations that are lower than at the front of the filter. Compounds will therefore tend to be stripped from the filtered particles. Pressure drop and ratio of the equilibrium vapor density of the aerosol species to its mass concentration are the dominant factors affecting evaporative loss rates (1). Volatilization of organic aerosol from the filter will lead to the underestimation of organic aerosol concentrations and comprises negative artifacts.

Whether adsorption or volatilization is the dominant sampling artifacts may depend on many factors, such as chemical nature of the sampled particles, concentration of vapor organic compounds, pressure drop across the filter, etc. Better understanding of these artifacts is very important in the measurement of organic aerosol concentrations.

4.1.2 Tandem filter method for correcting artifacts

A recommended method of correction for the positive artifacts involves sampling with a

backup filter. The organic content of the backup filter may provide an estimate of the adsorbed organic vapor on the front filter. This tandem filter method assumes that: (a) the amount of organic vapor adsorbed on the front and the backup filters are equal; (b) adsorption on the front filter but not evaporation from the front filter is the dominant sampling artifacts. Therefore, the adsorption sampling artifacts can be corrected by subtract the backup filter measurement from the front filter measurement. However, if the organic content of the backup filter is mainly from volatilization of particles on the front filter, the backup filter measurement should be added to the front filter measurement to correct the volatilization sampling artifacts.

4.1.3 Equilibrium between gas and adsorbed phases

The partitioning of organic compounds between gas and adsorbed phases on sampling filters is conceptually similar to gas-particle partitioning. The amount of organic vapor adsorbed on the filters will increase as sampling duration time increases until the equilibrium between gas and adsorbed phases is reached. In the tandem filter method, before the equilibrium is reached, the backup filter may not absorb as much organic vapor as the front filter, and therefore may not be able to provide a good estimate of the adsorbed organic vapor on the front filter. It can take a long time for partitioning to quartz filters to reach equilibrium. When quartz-quartz pair filters are used, it is observed that the tandem filter method under-corrects for the positive artifact if the sampling time is short (few hours) (2). Moreover, after the equilibrium between gas and adsorbed phases is reached, further increase of sampling duration will also reduce the percentage of collected material which is adsorbed vapor. Therefore, the accuracy of the method improves with increased sampling time (sampling volume). The precision of OC measurements was function of filter's carbon loading (3).

The minimum sampling volume required to reach gas/filter adsorption equilibrium with filters can be expressed as the product of partition coefficient, the filter face area and the number of filters. The minimum sampling volume will depend on chemical nature of the

compounds, relative humidity (RH), temperature, and filter type (4).

4.1.4 Measurement of OC in DPM

The measurement of OC/EC in DPM is often accomplished using particle collection on quartz fiber filters, followed by analysis using the thermal-optical method or one of its variations. Since the existing occupational exposure limits are based on the determination of EC, in practice it is not necessary to carry out a determination of OC. Less effort has been made to correct the sampling artifacts of OC in DPM in part due to the complexity of the task. In an international comparison study of DPM measurement, it is found that the inter-laboratory coefficient of variation for OC was approximately twice the coefficient of variation for EC (5).

Steven H. Cadle, et al has tried to use tandem filter method to measure OC in DPM (6). A PM10 sampler was used and the sampling flow rate is 28.3 L/min. Backup filters were collected for 20 samples. The amount of OC found on the backup filter was relatively insensitive to the front filter loading. Thus, the OC expressed as a percent of that found on the front filter varied from less than 1% for a heavily loaded sample to 34% for a lightly loaded sample. When quartz filters were run simultaneously behind both Teflon and quartz front filters, it was found that the quartz filters behind the Teflon collected twice as much carbon (28%) as those behind the quartz filters. Overall, it is concluded that quartz filters can capture substantially more OC than Teflon filters. However, since it is not well known that if all of the adsorbed OC was initially present in the gas phase, or if some of it was released from particles collected on the front filter, no corrections were made to the OC values reported from the quartz filters.

There have been many studies on organic aerosol sampling artifacts in the measurement of urban atmospheres (7-9). However, for the measurement of a specific source category, such as DPM sampling, related sampling issues are still under-explored. The organic matter associated with diesel emissions is an aggregate of hundreds of individual

compounds with a wide range of chemical and thermodynamic properties, and particulate organic matter constitutes approximately 20%-60% of DPM (10-13). In order to provide more accuracy in addressing health risks associated with DPM exposure, it is important to be able to quantify contributions of organic compounds to DPM.

4.2 Objective of the study

A high-volume sampling system was developed to collect enough mass in order to perform effective speciation analysis of organic compounds (such as PAHs, nitro-compounds and oxygenated compounds, etc) in ambient DPM exposure. The main objective of this study is to obtain better understanding of organic compounds sampling artifacts in DPM measurement for high volume applications. Experiments are designed to evaluate the relative magnitude of adsorption and volatilization sampling artifacts. Based on the experimental results, the study also tries to determine the minimum sampling volume (sampling duration time) required to attain organic gas-phase adsorbed-phase equilibrium on a previously clean quartz fiber filter. The information will be helpful to choose valid sampling duration time for field sampling in order to effectively correct sampling artifacts caused by adsorption.

4.3 The high volume sampling system

4.3.1 Development of the high volume sampling system

The drawing of the high volume sampling system is shown in Figure 4-1. A high volume blower (General Metal Works Model 2000) is used to draw air through the system. Quartz-quartz pair tandem filters with diameter of 90mm are used to collect DPM and correct associated adsorption sampling artifacts. The sampling flow rate is adjustable from 250 L/min to 350 L/min and is measured by an orifice meter. The orifice meter is calibrated by a Pitot tube with a PVC air duct (Length: about 3 feet, Inner diameter: 2 inches). The sampling inlet is about 1.4 m from ground. The whole sampling system is installed in a cart with wheels to make it easy to be moved.

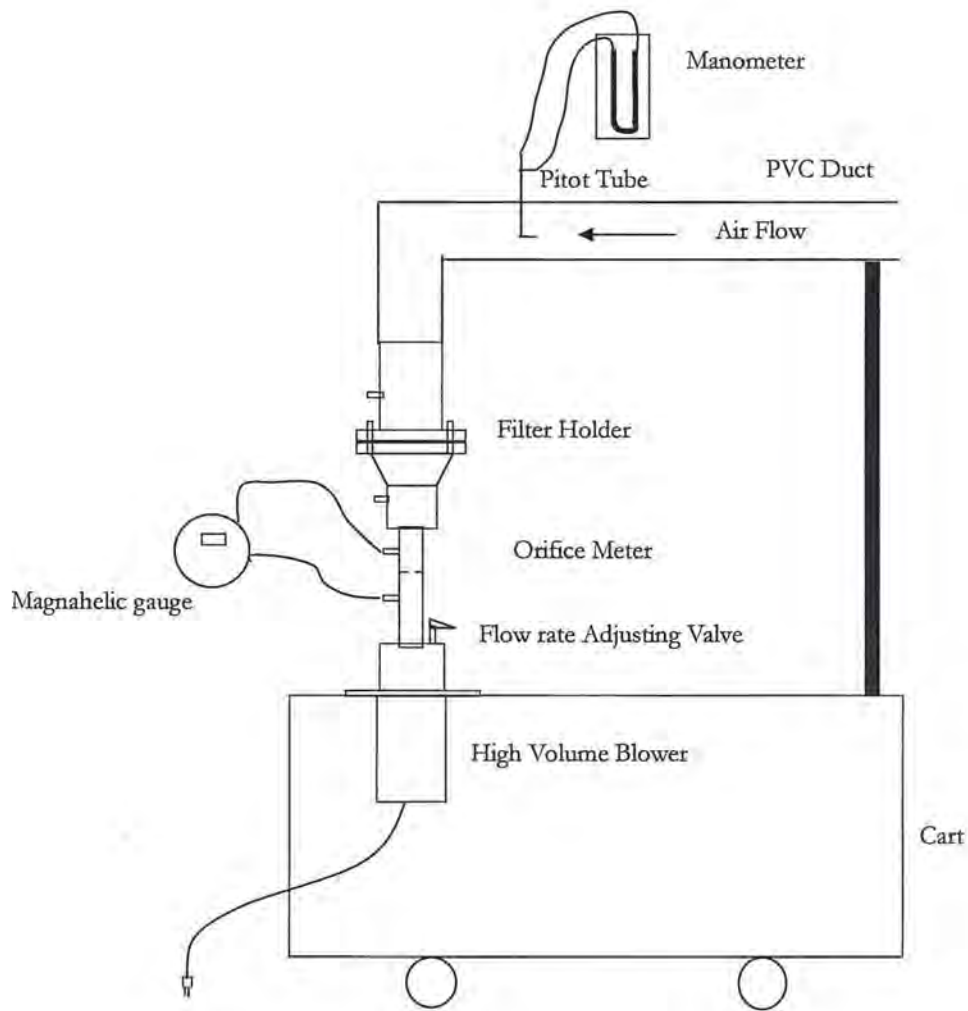


Figure 4-1 The high volume sampling system

4.3.2 Calibration of the flow rate

Pitot tube was used to calibrate orifice meter on the sampler. Parameters of calibration are listed in Table 4-1.

Table 4-1 Parameters of flow rate calibration

Ambient temperature during calibration, T_c (°F):	69
Ambient barometric pressure during calibration, P_c (in.Hg):	30.15
Relative humidity:	39%
Dew point (°F):	69
Molecular weight of air, M_c :	29
Diameter of PVC pipe (cm):	5.3

For Pitot tube, the air velocity can be calculated using the following equation:

$$V = 85.49 * [(T_c + 460) * \Delta H / P_c / M_c]^{0.5}, \text{ in feet/second.}$$

The calibration data of three high volume samplers are listed in Table 4-2.

Table 4-2 Calibration data of three high volume samplers

	ΔP of orifice (in. H ₂ O)	ΔH of pitot tube (in. H ₂ O)	Velocity (ft/s)	Velocity (cm/s)	Qcal, std (slpm)	$(\Delta P)^{1/2}$
#1 sampler	43	0.023	10.08	307.38	422.26	6.56
	31	0.016	8.41	256.37	352.19	5.57
	25.5	0.013	7.58	231.09	317.46	5.05
	22.5	0.012	7.28	222.03	305.01	4.74
	20	0.011	6.97	212.57	292.02	4.47
	17.5	0.01	6.65	202.68	278.43	4.18
	15	0.008	5.95	181.28	249.04	3.87
	11	0.006	5.15	157.00	215.67	3.32
#2 sampler	42	0.026	10.72	326.82	448.96	6.48
	30	0.018	8.92	271.93	373.56	5.48
	25.5	0.016	8.41	256.37	352.19	5.05
	19	0.013	7.58	231.09	317.46	4.36
	17.5	0.011	6.97	212.57	292.02	4.18
	15	0.01	6.65	202.68	278.43	3.87
	12.5	0.009	6.31	192.28	264.14	3.54
	10	0.008	5.95	181.28	249.04	3.16
#3 sampler	42	0.027	10.93	333.04	457.51	6.48
	41	0.027	10.93	333.04	457.51	6.40
	25	0.017	8.67	264.27	363.03	5.00
	24.5	0.016	8.41	256.37	352.19	4.95
	17	0.012	7.28	222.03	305.01	4.12
	16.5	0.011	6.97	212.57	292.02	4.06
	12.5	0.009	6.31	192.28	264.14	3.54

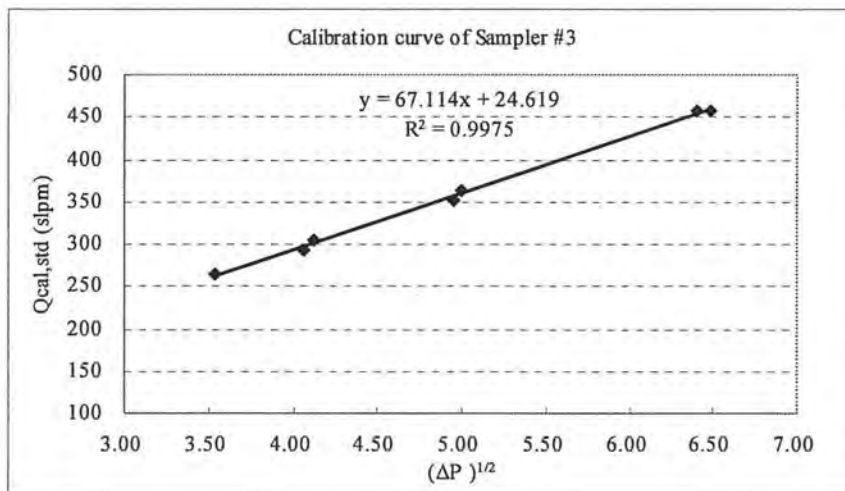
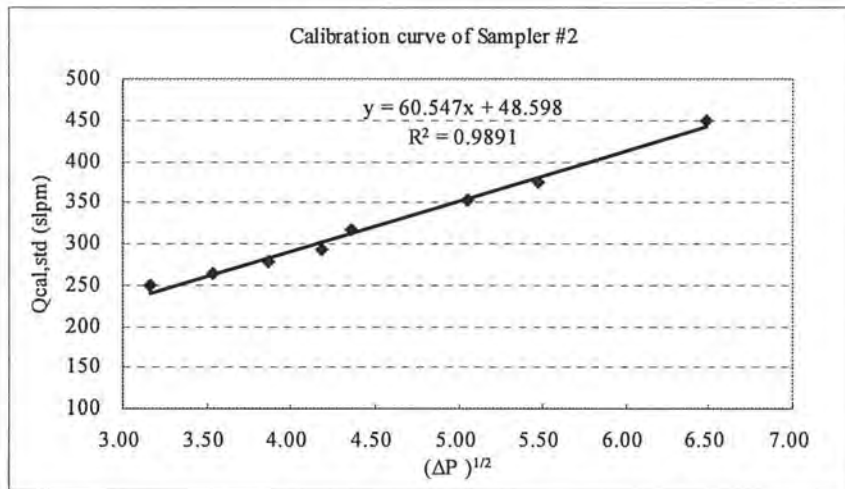
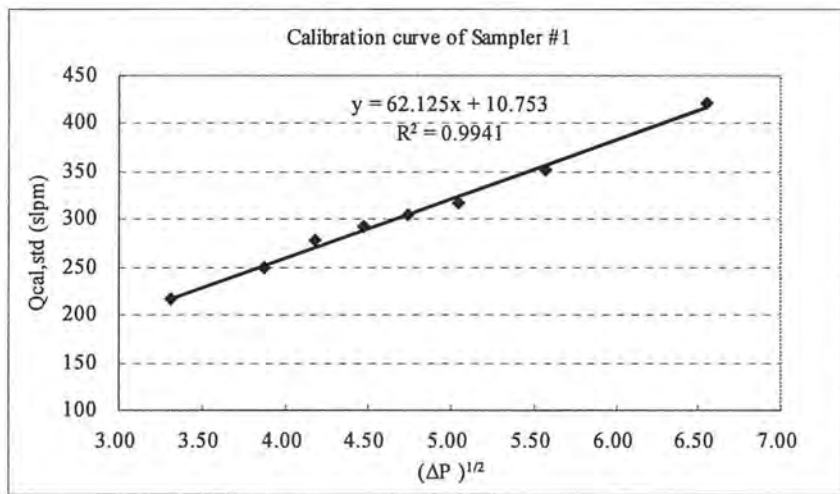


Figure 4-2 Calibration curve of the three high volume samplers

4.4 Experimental methods

The study was performed on a Generac diesel generator rated at 80 kW and 1800 rpm, which serves as a stationary DPM emission source. The high volume sampling systems were set up in vicinity of the generator to collect DPM samples in source influenced atmospheres, as shown in Figure 4-3. Quartz pair tandem filters (Millipore) were used to correct adsorption sampling artifacts. All quartz filters were baked at 700°C for at least 4 hours to remove carbon before sampling. Thermal analysis methods (NIOSH 5040) (14) were used to determine the OC and EC on the sampled filters. A punch from the sampled filter is taken for analysis, and OC and EC are reported in terms of μg per cm^2 of filter area. The total OC and EC on the filter are calculated by multiplying the reported values by the deposit area. Results of multiple punches from a single sampled filter show that sample deposit is homogeneous.

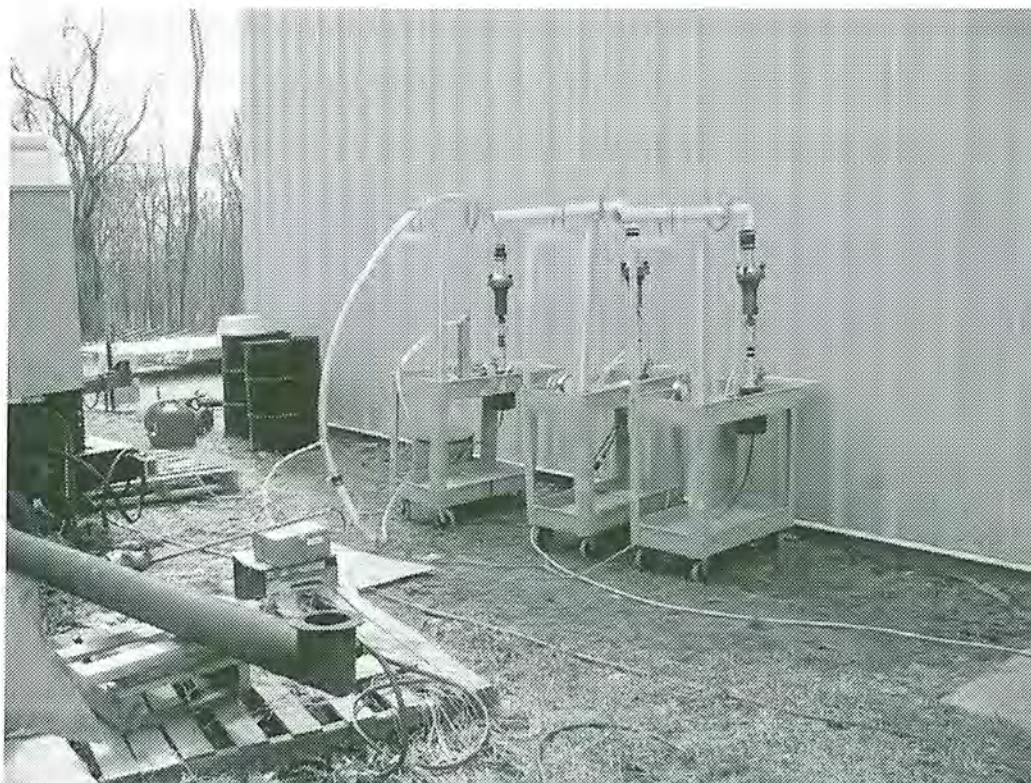


Figure 4-3 Picture of the high volume sampling system and the DPM emission source

Background samples were collected when the diesel generator was off and DPM influenced samples were all taken when the diesel generator was set at 0kW. Comparing the background samples and the DPM influenced samples, it was found that DPM occupies more than 82% of the total particulate concentration in DPM influenced samples. In order to study the sampling artifacts, DPM influenced samples were taken at two different filter face velocities (80cm/s and 105cm/s) and a series of collection time from 10 minutes to 600 minutes.

4.5 Results and discussions

4.5.1 Measurements of EC

EC is nonvolatile and therefore are believed not to be affected by sampling artifacts. No EC was found on the backup filter. Also, as expected, EC measurements are also not influenced by sampling conditions such as collection time and face velocity. Figure 4-4 shows the apparent OC and EC concentrations (based on the front filter measurement) at 105cm/s face velocity. It indicates that, while apparent OC concentration is obviously influenced by collection time, EC concentration does not show any relationship with collection time. The trend line of EC concentration vs. collection time has a slope as small as -0.0015. Data also shows that the relative percent deviation of EC of the simultaneous parallel samples taken at the two face velocities were from -3.60% to 8.01%.

Since EC measurements can reflect the actual DPM exposure level and not obviously affected by sampling artifacts, assuming OC/EC ratio is constant for the same source, EC was used to normalize the OC data so that samples at different DPM exposure level become comparable. All the OC data were normalized to the average EC concentration $3.76\mu\text{g}/\text{m}^3$.

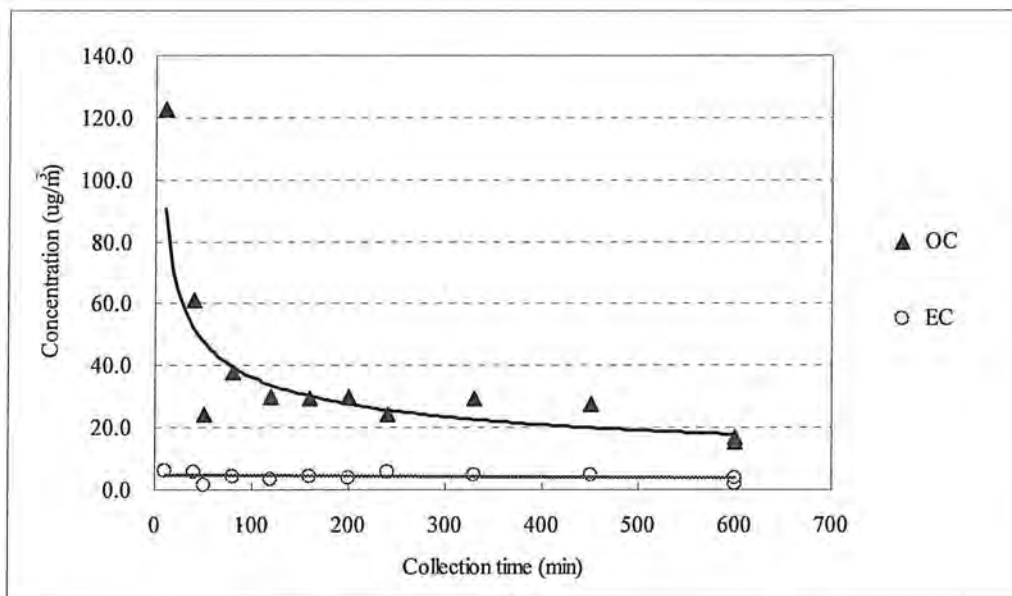


Figure 4-4 Apparent OC and EC concentrations based on the front filter measurement at 105cm/s face velocity

4.5.2 Dependency of OC measurements on collection time

Figure 4-5 shows the normalized apparent concentrations of OC based on the front filter measurement at the two different face velocities. It is found that, the apparent concentrations of OC decrease sharply as collection time increase. Since the actual particulate OC concentration should not be influenced by collection time, it indicates that sampling artifacts have great effect on the particulate OC measurement. As the collection time increase, the decrease of apparent concentrations of OC may caused by decrease of adsorbed OC vapor on the front filter, and it may also caused by the increase of volatilization of particles from the front filter.

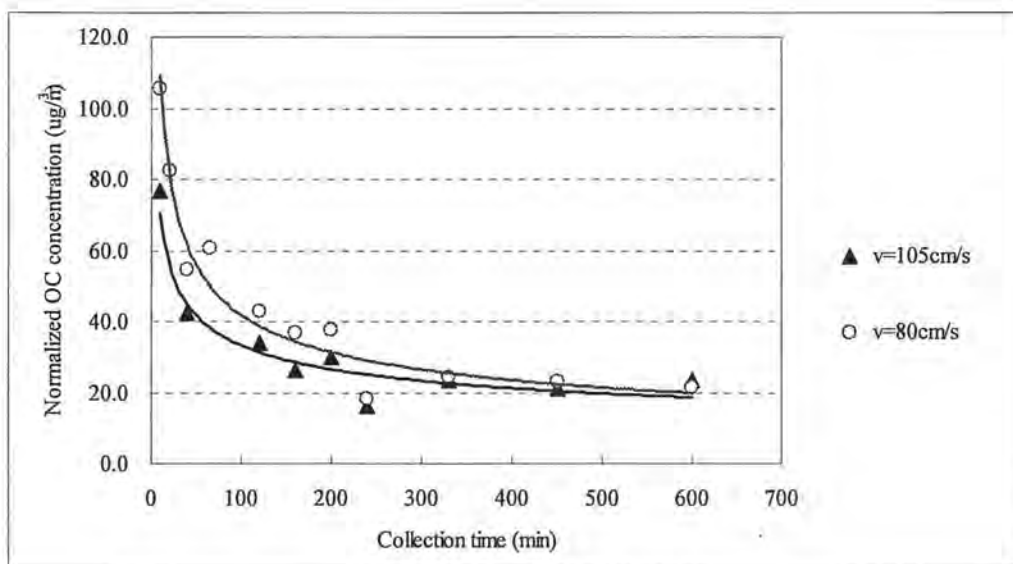


Figure 4-5 Normalized apparent concentrations of OC based on the front filter measurement at the two different face velocities

Figure 4-6 shows the normalized concentrations of OC vapor adsorbed on the backup filter at the two different face velocities. Since OC on the backup filter also decrease as collection time increase, when subtracting backup filter measurements from the front filter measurements, the dependency of OC on collection time was reduced. It can be concluded that OC on the backup filter was mainly from adsorption of vapor but not from volatilization of particles on front filter. Otherwise, they should increase as collection time increase, and the dependency of OC on collection time should be reduced by adding the backup filter measurements on the front filter measurements.

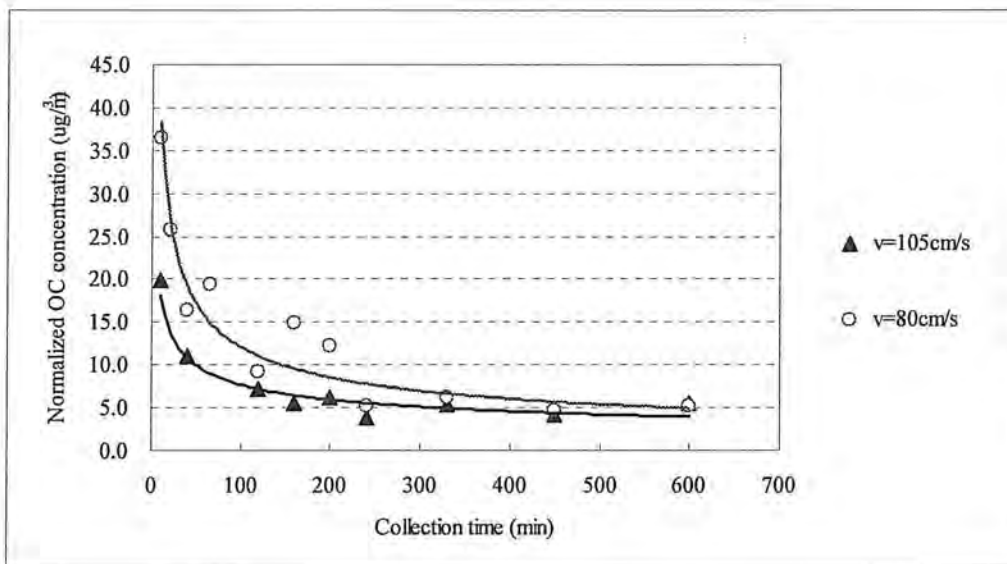


Figure 4-6 Normalized concentrations of OC vapor adsorbed on the backup filter at the two different face velocities

4.5.3 Dependency of OC measurements on face velocity

Moreover, Figure 4-5 and Figure 4-6 also shows that, when collection time is short (less than 300 min), both front filter and backup filter have obviously more OC at 80cm/s face velocity than that at 105cm/s face velocity. At lower face velocity, more OC vapor is adsorbed. When $v=80\text{cm/s}$, the average percentage of backup filter OC over front filter OC is 28.6% with a standard deviation of 6.1%. When $v=105\text{cm/s}$, the average percentage of backup filter OC over front filter OC is 22.8% with a standard deviation of 2.1%.

When subtracting backup filter measurements from the front filter measurements, the dependency of OC on face velocity can be reduced. It confirms the conclusion that, under the specified sampling conditions in the study, OC on the backup filter was mainly from adsorption of vapor but not from volatilization of particles on front filter. The quartz-quartz pair tandem filter method can be used to correct the adsorption artifacts by subtracting backup filter measurements from the front filter measurements.

4.5.4 Corrected OC concentrations

Figure 4-7 shows the corrected OC concentrations by subtracting backup filter measurements from the front filter measurements at the two different face velocities.

Figure 4-8 shows the difference of corrected OC at the two different face velocities [(OC at $v=80\text{cm/s}$)-(OC at $v=105\text{cm/s}$)]. It is found that, when the collection time is short (less than 300 min), the corrected OC concentrations still decrease as collection time increases and show a dependency on face velocity. One reason is that, in a short time the backup filters are not able to adsorb as much OC as the front filters, and therefore the adsorption artifacts are underestimated. Another reason is that, the volatilization artifacts are still not corrected.

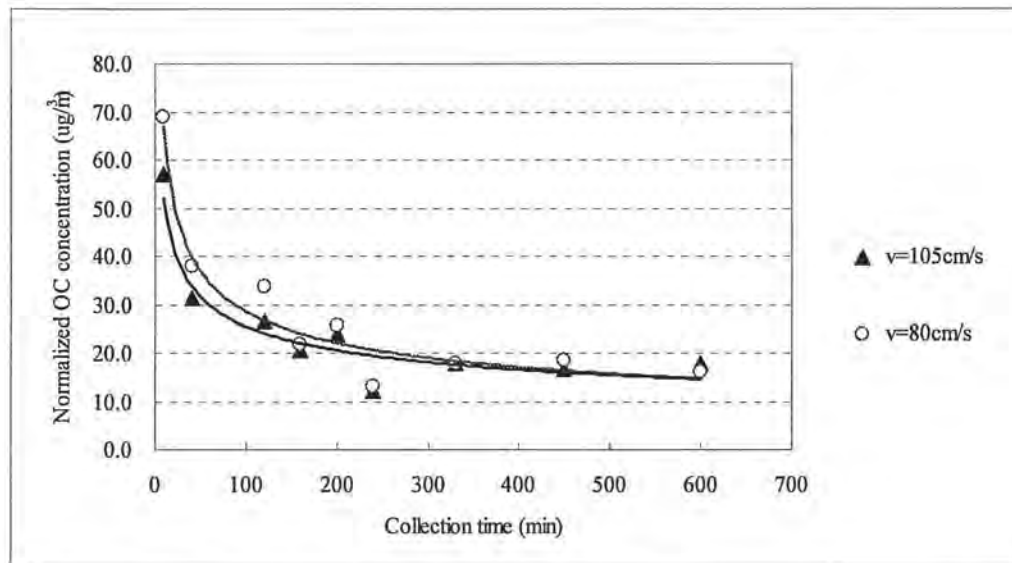


Figure 4-7 Corrected OC concentration by subtracting backup filter measurements from the front filter measurements at the two different face velocities

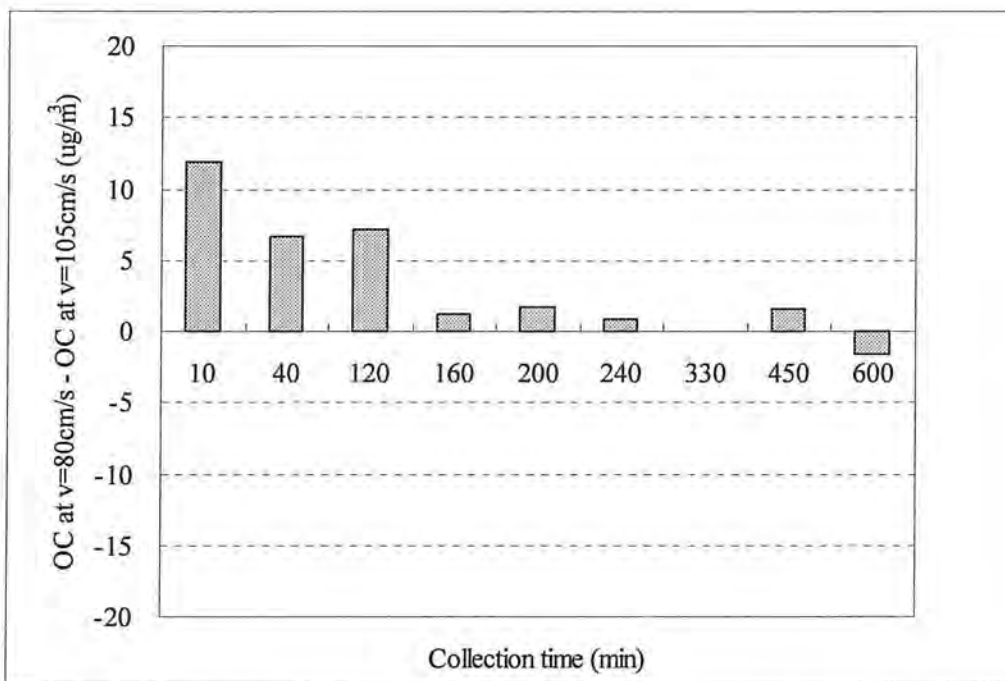


Figure 4-8 The difference of corrected OC at the two different face velocities
 $[(OC \text{ at } v=80\text{cm/s}) - (OC \text{ at } v=105\text{cm/s})]$

As collection time increase, the corrected OC concentrations become more and more stable, and the influences of face velocity become less and less important. It is believed that, when the equilibrium between gas and adsorbed phases is reached, the backup filters will be able to adsorb as much OC as the front filters, and the adsorption artifacts can be effectively corrected by subtracting backup filter measurements from the front filter measurements.

4.5.5 The gas/filter adsorption equilibrium

Figure 4-9 shows the OC loading (before normalization) on the backup filter along with the collection time. As we can see in the figure, when collection time was larger than 300min, OC loading on the backup filter did not increase much any longer, which indicates that the filters had approached their equilibrium to adsorb OC vapor. This finding agrees with what has been found from Figure 4-7 and Figure 4-8. Therefore, it can be concluded that, under the current sampling conditions, 300 min is the minimum

collection time in order to reach the gas/filter adsorption equilibrium and effectively correct the adsorption artifacts.

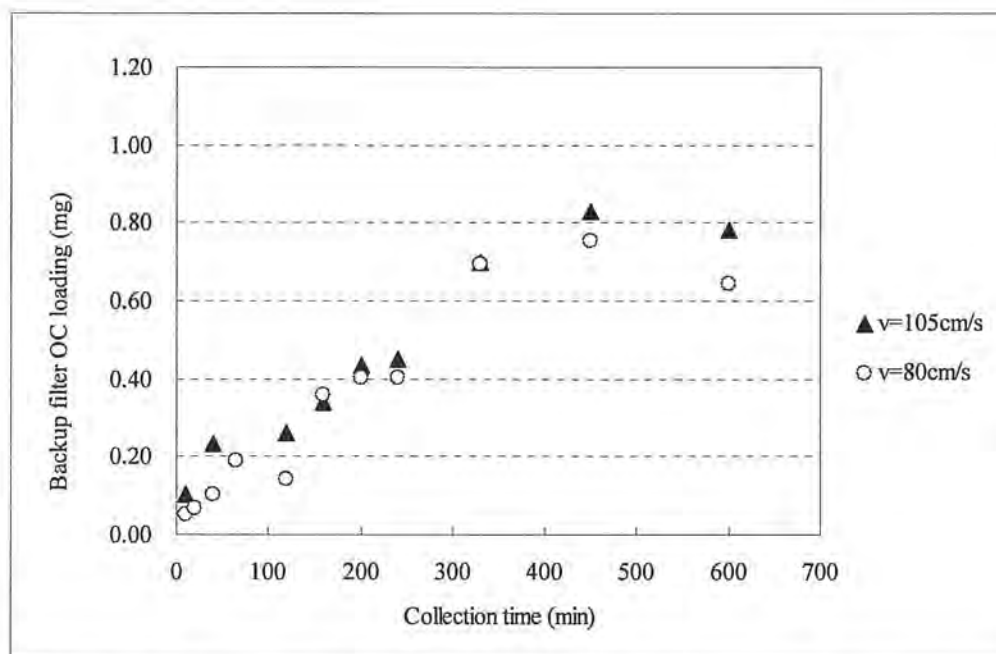


Figure 4-9 OC loading (before normalization) on the backup filter along with the collection time

In Figure 4-9, the maximum value of the adsorbed OC vapor on the backup filter is 0.83mg per filter (0.015mg per cm^2 filter area). In another test, Tandem filter method was evaluated when sampling source DPM using EPA Method 5 sampling train. Same quartz filters were used but with a diameter of 80mm (sampling area 48.99 cm^2) instead of 90mm (sampling area 53.52 cm^2). Figure 4-10 shows the OC loading on the filter along with the collection time in this Method 5 test. As can be seen in the figure, the adsorbed OC vapor on the backup filter reach equilibrium at about 30 min and has a maximum value of 0.67mg per filter (0.014mg per cm^2 filter area). The high-volume application test and the Method 5 test gave the similar value of the maximum OC vapor that can be adsorbed on the quartz filter when the gas/filter adsorption equilibrium is reached. In EPA Method 5 test, the filter face velocities were only 5.2cm/s to 5.8cm/s, which were

less than one tenth of that in the high-volume application test. It was found that the capability of quartz filter to adsorb OC vapor was not obviously influenced by sampling face velocity.

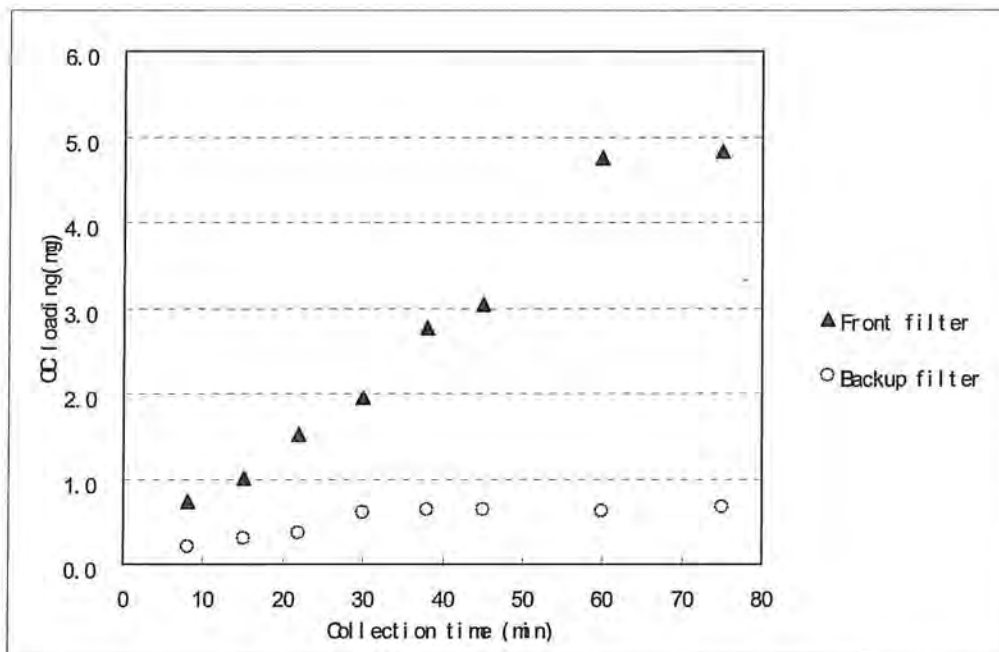


Figure 4-10 OC loading on the filter along with the collection time in the Method 5 test

4.6 Conclusion

The major conclusions obtained in this study include:

- Sampling artifacts have great influence in organic DPM measurement for high volume applications, especially when collection time is short.
- Under the specified sampling conditions in the study, OC on the backup filter was mainly from adsorption of vapor but not from volatilization of particles on front filter. The quartz-quartz pair tandem filter method can be used to correct the adsorption artifacts by subtracting backup filter measurements from the front filter measurements. The accuracy of the method improves with increased collection time.
- At lower face velocity, quartz filter tends to adsorb more OC vapor than at higher face velocity. In our test, When $v=105\text{cm/s}$, the average percentage of backup filter

OC over front filter OC was 22.8% with a standard deviation of 2.1%. When $v=80\text{cm/s}$, the average percentage of backup filter OC over front filter OC was 28.6% with a standard deviation of 6.1%. As collection time increases, the difference caused by different face velocities decreases.

- In order to effectively correct the adsorption artifacts, collection time should be long enough to approach gas/filter adsorption equilibrium. In our high volume sampling application, the minimum collection time is about 300 minutes.
- The capability of the applied quartz filter (Millipore) to adsorb OC vapor was not obviously influenced by sampling face velocity.

Partial results of this study have been presented on the American Association for Aerosol Research (AAAR) 2004 Annual Conference.

4.7 References

- (1). Turpin, B.J.; Saxena, P.; Andrews, E. Measuring and simulating particulate organics in the atmosphere: problems and prospects, *Atmospheric Environment*, 2000, 34, 2983-3013.
- (2). Kirchstetter, T.W.; Corrigan, C.E.; Novakov, T. Laboratory and field investigation of the adsorption of gaseous organic compounds onto quartz filters, *Atmospheric Environment*, 2001, 35, 1663-1671.
- (3). Schauer, J. J.; Mader, B. T.; DeMinter, J. T.; Heidemann, G.; Bae, M. S.; Seinfeld, J. H.; Flagan, R. C.; et. al. ACE-Asia inter-comparison of a Thermal-Optical Method for the Determination of Particle-Phase Organic and Elemental Carbon, *Environ. Sci. Technol.*, 2003, 37(5), 993-1001.
- (4). Mader B.T. and Pankow. J.F. Gas/solid partitioning of semi-volatile organic compounds (SOCs) to air filters 3, *Environ. Sci. Technol.*, 2001, 35(17), 3422-3432.
- (5). Heibisch, R.; Dabill, D.; Dahmann, D.; Diebold, F.; Geiregat, N.; Grosjean, R.; Mattenklott, M.; Perret, V.; Guillemin, M. Sampling and analysis of carbon in diesel

- exhaust particulates - an international comparison, *INTERNATIONAL ARCHIVES OF OCCUPATIONAL AND ENVIRONMENTAL HEALTH*, 2003, 76(2), 137-142.
- (6). Cadle, S.H.; Nelson, K.; Ragazzi, R.A.; Barrett, R.; Gallagher, G.L.; Lawson, D.R.; Knapp, K.T.; Snow, R. Composition of Light-Duty Motor Vehicle Exhaust Particulate Matter in the Denver, *Environ. Sci. Technol.* 1999, 33(14), 2328-2339.
- (7). Turpin B.J. and Huntzicker, J.J. Investigation of organic aerosol sampling artifacts in the Los Angeles Basin, *Atmospheric Environment*, 1994, 28(19), 3061-3071.
- (8). Zhang, X.Q. and McMurry, P.H. Theoretical analysis of evaporative losses from impactor and filter deposits, *Atmospheric Environment*, 1987, 21(8), 1779-1789.
- (9). Hart K.M. and Pankow, J.F. High-Volume air sampler for particle and gas sampling. 2. Use of backup filter to correct for the adsorption of gas-phase polycyclic aromatic hydrocarbons to the front filter, *Environ. Sci. Technol.*, 1994, 28(4), 655-661.
- (10). Shi, J.P.; Mark, D.; Harrison, R.M. Characterization of Particles from a Current Technology Heavy-Duty Diesel Engine, *Environ. Sci. Technol.* 2000, 34 (5), 748-755.
- (11). Kerminen, V.M.; Makela, T.E.; Ojanen, C.H.; Hillamo, R.E. Characterization of the particulate phase in the exhaust from a diesel car, *Environ. Sci. Technol.* 1997, 31(7), 1883-1889.
- (12). Rogers, F.C.; Sagebiel, J.C.; Zielinska, B.; Arnott, P.W.; Fujita E.M.; McDonald, J.D.; Griffin, J.B.; Kelly, K.E.; Overacker, D.; Wagner, D.; Lighty, J.S.; Sarofim, A.; Palmer, G. Characterization of Submicron Exhaust Particles from Engines Operating Without Load on Diesel and JP-8 Fuel, *Aerosol Sci. Tech.* 2003, 37, 355-368.
- (13). Kelly, K.E.; Wagner, D.A.; Lighty, J.S.; Sarofim, A.F. Characterization of Exhaust Particles from Military Vehicles Fueled with Diesel, Gasoline, and JP-8. *J. Air & Waste Manage. Assoc.* 2003, 53(3), 273-282.
- (14). U.S. Department of Health and Human Services (DHHS), Public Health Service, Centers for Disease Control, National Institute for Occupational Safety and Health (NIOSH). NIOSH Manual of Analytical Methods (*NMAM*), Cassinelli, M.E., O'Connor, P.F., Eds. Second Supplement to *NMAM*, 4th Edition. Publication No. 94-113. Cincinnati, OH. 1998.

Chapter 5 Recommendations for Future Work

In this study, investigation of carbon and sulfur speciation of diesel emissions were all based on undiluted samples directly from the stack. However, the dilution process has great influence on the speciation of diesel emissions. In order to obtain understanding of the effect of dilution process on DPM compositional variations, it would be interesting to compare the carbon and sulfur speciation information from diluted samples and undiluted samples. For example, OC in DPM may be generated directly from unburned fuel and lube oil, and it may be also from nucleation and condensation of organic vapor during secondary processes such as dilution. And sulfate is supposed to play an important role in the nucleation and condensation of OC. In Figure 3-4, a "U" type trend along with engine loads has been found for sulfate, and it may help to explain the similar "U" type trend which has been found for condensed organic compounds in Figure 2-10. By comparing diluted samples and undiluted samples at various diesel sulfur content and various loads, better understanding of the OC, EC and sulfate distribution and their relationship can be obtained.

In the sulfur speciation study, the sulfur recovery is sensitive to diesel fuel types. This may indicate that some types of diesel fuels have more sulfur not oxidized in their emissions. Also, the highest sulfur recoveries were achieved at 0kW load for all the diesel fuels. It would be interesting to look for other sulfur compounds in diesel emissions when sulfur recovery is low. It may be reduced sulfur, organic sulfur compounds in vapor phase which were not measured in this study. It is found that, the sulfur compounds in the high sulfur diesel (S=2200ppm) were obviously different with that in other three diesel fuels. It may relate to its obviously low sulfur recovery. In order to identify the key parameters that influence the sulfur recovery, further investigation on more types of diesel would be helpful.

The SEM images may be able to provide visual aid to understand how dilution process,

engine load, and diesel sulfur content may influence the DPM morphology. Some preliminary study on SEM (Scanning Electron Microscopy) images of DPM has been done and is shown in Appendix D. It is found that, DPM does have different look at 0kW and at 75kW. And on images of diluted samples, obvious condensation can be identified as compare with undiluted samples. Further investigations on SEM images of DPM as a function of diesel sulfur content, engine load and dilution condition are needed for better clarification.

Appendix A: Data sheet of OC/EC study in Chapter 2

Sampling conditions	Load (kW)	flow rate (l/min)	Total OC (mg)	Total EC (mg)	Total TC (mg)	Sample volume (m3)	Total DPM (mg)	OC Conc. (mg/m3)	OC*1,2 Conc. (mg/m3)	EC Conc. (mg/m3)	TC Conc. (mg/m3)	DPM Conc. (mg/m3)	OC*1,2 /DPM	EC /DPM	(OC*1,2 +EC) /DPM	OC/EC
S = 500ppm, T = 120 °C ± 14 °C	0	19.2	0.4064	0.1687	0.5750	0.2883	0.79	1.41	1.69	0.58	1.99	2.74	62%	21%	83%	2.41
	25	20.1	0.6590	0.5200	1.1790	0.3009	1.53	2.19	2.63	1.73	3.92	5.08	52%	34%	86%	1.27
	50	21.0	0.7703	1.2261	1.9964	0.3144	2.35	2.45	2.94	3.90	6.35	7.48	39%	52%	92%	0.63
	75	23.6	0.1348	1.4897	1.6245	0.1888	1.77	0.71	0.86	7.89	8.61	9.38	9%	84%	93%	0.09
S = 3700ppm, T = 120 °C ± 14 °C	0	18.7	1.4291	0.0972	1.5262	0.2803	2.23	5.10	6.12	0.35	5.44	7.96	77%	4%	81%	14.71
	25	19.1	1.5831	0.2946	1.8776	0.2867	2.87	5.52	6.63	1.03	6.55	10.01	66%	10%	76%	5.37
	50	15.1	1.5577	0.3888	1.9466	0.2263	2.74	6.88	8.26	1.72	8.60	12.11	68%	14%	82%	4.01
	75	22.6	0.4301	1.5008	1.9309	0.1811	2.75	2.37	2.85	8.29	10.66	15.18	19%	55%	73%	0.29
S = 500ppm, T = 25 °C ± 3 °C	0	16.0	1.0620	0.1785	1.2405	0.2395	1.69	4.44	5.32	0.75	5.18	7.06	75%	11%	86%	5.95
	25	16.1	1.0729	0.3836	1.4565	0.2411	1.99	4.45	5.34	1.59	6.04	8.25	65%	19%	84%	2.80
	50	16.2	0.9278	0.9521	1.8799	0.2436	2.49	3.81	4.57	3.91	7.72	10.22	45%	38%	83%	0.97
	75	16.9	0.9270	2.4835	3.4104	0.2529	4.18	3.67	4.40	9.82	13.49	16.53	27%	59%	86%	0.37

Appendix B: Data sheet of sulfur speciation study in Chapter 3

Diesel Sulfur content	Load (kW)	excess air	Concentration (mg/dscm)					Particulate Sulfate-S/TPS	Fuel consumption rate (L/hr)	Flue gas rate (dscm/hr)	Sulfur recovery rate (%)	Sulfur Conversion Rate (%)				Vapor SO4/Total SO4	
			SO2	H2SO4	Particulate Sulfur		Particulate Sulfate-S/TPS					Particulate Sulfur		SO2-S	H2SO4-S		
					Sulfate	TPS	TPS					Sulfate-S	TPS				Sulfate-S
300ppm	0	5.60	4.43	3.69	0.046	0.014	109.5%	5.0	350	96.9%	0.40%	0.43%	62.49%	34.00%	98.74%		
300ppm	25	2.70	8.15	1.63	0.054	0.034	52.9%	10.0	363	67.9%	0.50%	0.26%	59.62%	7.79%	96.73%		
300ppm	40		11.52	1.90	0.085			13.0	348			0.31%	62.15%	6.69%	95.63%		
300ppm	50	1.95	12.03	1.48	0.07	0.046	50.7%	15.0	380	66.8%	0.47%	0.24%	61.42%	4.93%	95.39%		
300ppm	50	1.95	11.72	1.57	0.074			15.0	357			0.24%	56.21%	4.92%	95.41%		
300ppm	60		13.49	0.94	0.09			17.0	357			0.25%	57.09%	2.60%	91.10%		
300ppm	75	1.45	14.49	2.01	0.105	0.061	57.4%	19.5	396	65.2%	0.50%	0.29%	59.30%	5.37%	94.94%		
400ppm	0	5.60	8.01	3.76	0.031			5.0	328			0.20%	79.42%	24.35%	99.17%		
400ppm	0	5.60	7.25	4.87	0.037	0.012	100.2%	5.0	349	110.3%	0.26%	0.26%	76.49%	33.55%	99.23%		
400ppm	25	2.70	14.47	2.02	0.061	0.026	78.6%	10.0	342	81.9%	0.27%	0.21%	74.80%	6.82%	97.01%		
400ppm	50	1.95	20.19	2.91	0.077	0.047	54.7%	15.0	351	78.5%	0.33%	0.18%	71.41%	6.72%	97.37%		
400ppm	75	1.45	24.52	3.36	0.116	0.070	55.3%	19.5	389	81.0%	0.42%	0.23%	73.93%	6.62%	96.60%		

(to be continued)

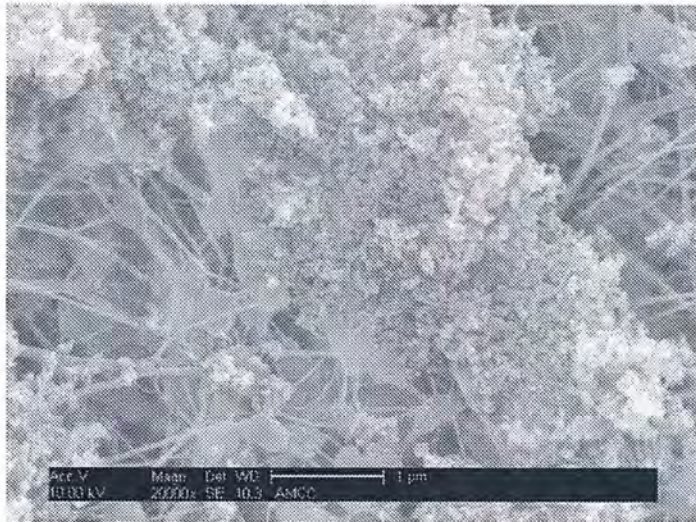
Diesel Sulfur content	Load (kW)	excess air	Concentration (mg/dscm)					Particulate Sulfate-S/TPS	Fuel consumption rate (L/hr)	Flue gas rate (dscm/hr)	Sulfur recovery rate (%)	Sulfur Conversion Rate (%)				Vapor SO4/Total SO4	
			SO2	H2SO4	Particulate Sulfur		Particulate Sulfur					TPS	Sulfate-S	SO2-S	H2SO4-S		
					Sulfate	TPS	TPS										Sulfate-S
450ppm	0	5.60	9.58	2.07	0.059			5.0	340			0.36%	87.52%	12.35%	97.17%		
450ppm	0	5.60	9.36	2.19	0.056	0.021	88.9%	5.0	340	99.0%	0.38%	0.34%	85.51%	13.07%	97.46%		
450ppm	10		15.50	1.59	0.049			7.0	367			0.23%	109.18%	7.31%	96.95%		
450ppm	25	2.70	17.43	1.90	0.041			10.0	337			0.12%	78.92%	5.62%	97.84%		
450ppm	25	2.70	18.75	1.32	0.05	0.023	72.5%	10.0	349	92.2%	0.22%	0.16%	87.92%	4.04%	96.28%		
450ppm	25	2.70	17.92	1.86	0.063			10.0	354			0.20%	85.23%	5.78%	96.66%		
450ppm	40		19.99	1.60	0.054			13.0	350			0.13%	72.31%	3.78%	96.67%		
450ppm	50	1.95	26.67	1.38	0.083			15.0	339			0.17%	80.98%	2.74%	94.22%		
450ppm	50	1.95	25.03	1.42	0.083	0.053	52.2%	15.0	357	83.3%	0.34%	0.18%	80.04%	2.97%	94.37%		
450ppm	50	1.95	23.58	1.17	0.102			15.0	368			0.22%	77.72%	2.52%	91.83%		
450ppm	60		28.04	1.57	0.089			17.0	362			0.17%	80.22%	2.93%	94.53%		
450ppm	75	1.45	30.79	1.71	0.123	0.077	53.2%	19.5	382	84.4%	0.41%	0.22%	81.04%	2.94%	93.16%		
450ppm	75	1.45	29.77	2.66	0.106			19.5	394			0.19%	80.82%	4.72%	96.09%		
2200ppm	0	5.60	30.06	2.63	0.074			5.0	341			0.09%	56.34%	3.22%	97.21%		
2200ppm	0	5.60	32.04	1.96	0.065			5.0	302			0.07%	53.18%	2.12%	96.73%		
2200ppm	0	5.60	36.21	2.90	0.061	0.040	50.5%	5.0	340	71.4%	0.15%	0.08%	67.67%	3.54%	97.90%		
2200ppm	25	2.70	56.20	3.52	0.108	0.063	56.9%	10.0	350	56.4%	0.12%	0.07%	54.06%	2.21%	96.96%		
2200ppm	25	2.70	56.71	3.62	0.113			10.0	299			0.06%	46.60%	1.94%	96.91%		
2200ppm	50	1.95	78.64	2.84	0.208			15.0	352			0.09%	50.72%	1.20%	93.04%		
2200ppm	50	1.95	80.89	3.79				15.0	358				53.06%	1.62%			
2200ppm	50	1.95	79.48	2.19	0.226	0.120	62.7%	15.0	354	52.6%	0.16%	0.10%	51.55%	0.93%	90.47%		
2200ppm	75	1.45	97.80	4.77				19.5	367				50.58%	1.61%			
2200ppm	75	1.45	99.56	3.84	0.238	0.129	61.5%	19.5	389	56.1%	0.14%	0.09%	54.58%	1.37%	94.05%		
2200ppm	75	1.45	97.57	4.69	0.362			19.5	343			0.12%	47.16%	1.48%	92.70%		

Appendix C: Data sheet of sampling artifacts study in Chapter 4

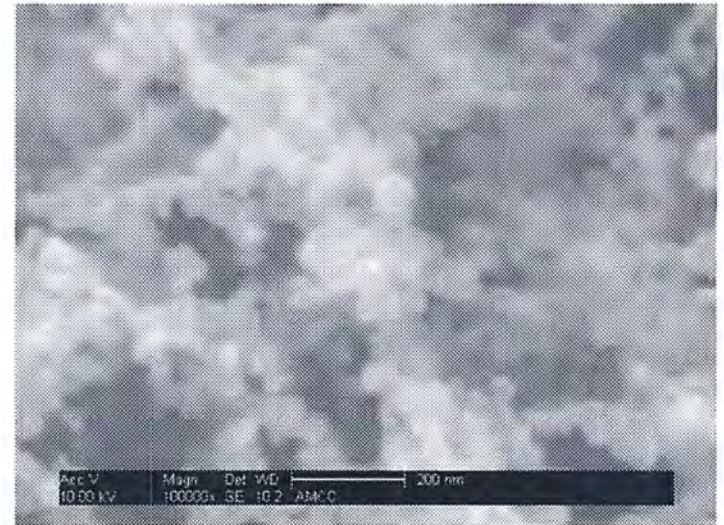
Filter face velocity (cm/s)	sampling time (min)	T (°F)	P _b (in. Hg)	Sampling volume (m ³)	Total OC(mg)		Total EC(mg)		OC Conc (ug/m ³)		EC Conc(ug/m ³)		OC Conc. normalized by EC (ug/m ³)		Back OC /Front OC
					front	back	front	back	front	back	front	back	front	back	
					filter	filter	filter	filter	filter	filter	filter	filter	filter	filter	
105	10	80.8	29.43	3.23	0.3971	0.1025	0.0194	0.0000	122.88	31.70	6.00	0	76.91	19.84	25.80%
108	40	51.0	30.16	14.51	0.8895	0.2324	0.0787	0.0000	61.30	16.02	5.42	0	42.45	11.09	26.13%
105	120	55.0	29.53	40.86	1.2286	0.2611	0.1363	0.0000	30.07	6.39	3.34	0	33.85	7.19	21.25%
107	160	55.0	29.53	55.39	1.6246	0.3403	0.2336	0.0000	29.33	6.14	4.22	0	26.12	5.47	20.94%
108	200	55.0	29.53	70.12	2.1021	0.4349	0.2626	0.0000	29.98	6.20	3.75	0	30.07	6.22	20.69%
105	240	75.0	29.20	77.79	1.8889	0.4513	0.4426	0.0000	24.28	5.80	5.69	0	16.03	3.83	23.89%
105	330	84.5	29.28	105.38	3.0857	0.6994	0.4967	0.0000	29.28	6.64	4.71	0	23.33	5.29	22.67%
105	450	59.0	29.20	150.35	4.1242	0.8274	0.7348	0.0000	27.43	5.50	4.89	0	21.08	4.23	20.06%
105	600	71.0	29.50	197.95	3.3027	0.7818	0.3851	0.0000	16.68	3.95	1.95	0	32.22	7.63	23.67%
105	600	71.0	28.20	189.23	2.8857	0.6655	0.7463	0.0000	15.25	3.52	3.94	0	14.52	3.35	23.06%
72	10	80.8	29.43	2.21	0.1537	0.0532	0.0055	0.0000	69.46	24.03	2.47	0	105.48	36.49	34.60%
80	20	80.7	29.40	4.96	0.2096	0.0656	0.0096	0.0000	42.27	13.23	1.93	0	82.24	25.75	31.31%
72	40	88.8	29.24	8.66	0.3361	0.1011	0.0232	0.0000	38.79	11.67	2.68	0	54.42	16.36	30.07%
80	65	78.0	29.24	16.11	0.5906	0.1900	0.0367	0.0000	36.67	11.80	2.28	0	60.50	19.46	32.17%
76	120	80.0	29.24	27.89	0.6522	0.1402	0.0570	0.0000	23.39	5.03	2.04	0	43.00	9.24	21.50%
86	160	80.0	29.24	42.07	0.8932	0.3608	0.0915	0.0000	21.23	8.58	2.17	0	36.69	14.82	40.39%
82	200	80.8	29.43	50.45	1.2551	0.4040	0.1251	0.0000	24.88	8.01	2.48	0	37.70	12.13	32.19%
80	240	75.0	29.20	59.43	1.4206	0.4043	0.2914	0.0000	23.90	6.80	4.90	0	18.31	5.21	28.46%
75	330	84.5	29.28	75.18	2.6862	0.6933	0.4159	0.0000	35.73	9.22	5.53	0	24.26	6.26	25.81%
78	450	59.0	29.20	111.43	3.7285	0.7547	0.6050	0.0000	33.46	6.77	5.43	0	23.15	4.69	20.24%
80	600	71.0	29.50	151.96	2.6147	0.6428	0.3454	0.0000	17.21	4.23	2.27	0	28.43	6.99	24.58%
79	600	71.0	28.20	141.82	2.2381	0.5110	0.5853	0.0000	15.78	3.60	4.13	0	14.36	3.28	22.83%

Appendix D: SEM image of DPM

Undiluted samples on Teflon filter
Diesel sulfur content=2200ppm, load: 75kW,



20,000×



100,000×

Undiluted samples on Teflon filter
Diesel sulfur content=2200ppm, load: 0kW,



20,000×



100,000×

Diluted samples on Quartz filter
Diesel sulfur content=400ppm, load: 0kW,



5,000×



100,000×